Biochimica et Biophysica Acta 1865 (2017) 565–577

Contents lists available at ScienceDirect

Biochimica et Biophysica Acta

journal homepage: www.elsevier.com/locate/bbapap

Review

A structural appraisal of sterol carrier protein 2

Noelia I. Burgardt [a,1], Alejo R. Gianotti [b,1], Raúl G. Ferreyra [b], Mario R. Ermácora [b,*]

[a] Instituto de Química y Fisicoquímica Biológicas, UBA, CONICET, FFyB, Argentina
[b] Grupo Vinculado de Biología Estructural y Biotecnología, Universidad Nacional de Quilmes, IMBICE, CIC, UNLP, CONICET, Argentina

ARTICLE INFO

Article history:
Received 21 December 2016
Received in revised form 3 March 2017
Accepted 7 March 2017
Available online 08 March 2017

Keywords:
Sterol carrier protein 2
Lipid binding protein
Enhanced intracellular survival protein
Alkyl sulfatase
Non-specific lipid-transfer protein
MycE methyltransferase

ABSTRACT

Sterol Carrier Protein 2 (SCP2) has been associated with lipid binding and transfer activities. However, genomic, proteomic, and structural studies revealed that it is an ubiquitous domain of complex proteins with a variety functions in all forms of life. High-resolution structures of representative SCP2 domains are available, encouraging a comprehensive review of the structural basis for its success. Most SCP2 domains pertain to three major families and are frequently found as stand-alone or at the C-termini of lipid related peroxisomal enzymes, acetyltransferases causing bacterial resistance, and bacterial environmentally important sulfatases. We (1) analyzed the structural basis of the fold and the classification of SCP2 domains; (2) identified structure-determined sequence features; (3) compared the lipid binding cavity of SCP2 and other lipid binding proteins; (4) surveyed proposed mechanisms of SCP2 mediated lipid transfer between membranes; and (5) uncovered a possible new function of the SCP2 domain as a protein-protein recognition device.

1. Introduction

A long standing tenet in biochemistry is that there are specialized, non-catalytic, soluble, lipid-binding proteins that facilitate lipid storage, traffic, signaling, and metabolisms within the cell. This notion arose to reconcile the sparing water solubility of most lipids with biophysical mechanisms –such as binding and specific recognition– that involve dissolved molecules in aqueous phases.

The idea of 'Lipid Binding Proteins' (LBP) as lipid carriers and deposits appeared in the early 1970s [1], and since it has been the inspiration for a large number of investigations. These investigations provided clear and definitive evidence of the in vitro activity of many different soluble LBP. However, their in vivo activity turned to be much more difficult to establish and is the subject of intense debate. This difficulty is likely due to the multiplicity of soluble LBP in the cell and the redundancy of their action, which makes almost impossible to ascribe an specific functional effect to a single protein. The issue was recently reviewed [2–4].

Because of its ubiquity, binding properties, and tendency to be in multidomain proteins, the SCP2 domain is prominent among LBP. The discovery of SCP2 was the result of early efforts to identify and characterize cytosolic factors required for the microsomal synthesis of cholesterol and enhanced transfer of phospholipids between membranes. Since this protein –purified from rat tissues– was characterized independently by four different groups, it was also named 'non-specific Lipid-Transfer Protein' (nsLTP) or 'nonspecific-phospholipid-transfer protein' [5–8]. Unfortunately, the name 'non-specific lipid transfer protein' was later also used to identify an unrelated family of plant LBP, which constitutes a frequent source of confusions [9].

As the study of SCP2 progressed, its capacity of binding with high affinity to many different lipids was unveiled. It also became apparent that SCP2 may have many roles beyond binding sterols or transfer phospholipids in mammals, and it is found lone (unfused) or in a large variety of multidomain proteins in bacteria, archaea, and all kind of eukaryotes.

In eukaryotes, SCP2 is present at the C-termini of peroxisomal enzymes involved in beta oxidation of straight and 2-methyl-branched-chain fatty acyl-CoAs. One of these, peroxisomal multifunctional enzyme type 2, possesses, besides SCP2, enoyl-CoA hydratase and a (3*R*)-hydroxyacyl-CoA dehydrogenase domains. Another, peroxisomal 3-oxoacyl-CoA thiolase has a C-terminal SCP2 domain. In both, SCP2 seems to be crucial for peroxisome import.

SCP2 are especially relevant in bacteria. 'Eis' (Enhanced Intracellular Survival) proteins are versatile acetyltransferases that acetylate amines at multiple positions of aminoglycosides, inactivating them and causing bacteria resistance [10–12]. These proteins have three domains, two are GNAT N–acetyltransferase domains and the third is a C-terminal SCP2.

Abbreviations: SCP2, Sterol Carrier Protein 2; plm-pyr-pCho, 1-palmitoyl-2-[6-(1-pyrenyl)-hexanoyl] -sn-glycero-3-phosphocholine; NBD cholesterol, 22-(N-(7-nitrobenz-2-oxa-1,3-diazol-4-yl)amino)-23,24-bis nor-5-cholen-3β-ol; Pyr-lauric acid, pyrene lauric acid; Pyr-cholesterol, pyrene cholesterol; AO-palmitic acid, 2-(9-anthroyloxy)palmitatic acid; NBD-sphingomyelin, 6-((N-(7-nitrobenz-2-oxa-1,3-diazol-4-yl)amino)-hexanoyl)sphingosyl-phosphocholine; GM1, monosialotetrahexosylganglioside; SCPI-1, N -(4-{[4-(3,4-dichlorophenyl)-1,3-thiazol-2-yl]amino}phenyl)acetamide hydrobromide.

* Corresponding author at: Universidad Nacional de Quilmes, Roque Sáenz Peña 325, (1876), Bernal, Buenos Aires, Argentina.
E-mail address: ermacora@unq.edu.ar (M.R. Ermácora).

[1] These authors contributed equally to this work.

http://dx.doi.org/10.1016/j.bbapap.2017.03.002
1570-9639/

In them SCP2 contributes its C–terminal carboxylate to the catalytic mechanism of the acetylase domain. Eis homologues are present in diverse bacteria, including many pathogens and are the subject of a very intense research aimed to identify drugs inhibitors for clinical use [13].

Another example of multidomain bacterial proteins containing a SCP2 domain are alkyl sulfatases, which posses: a N–terminal catalytic domain with a binuclear Zn^{2+} cluster pertaining to the metallo–lactamase family, a dimerization domain, and a C–terminal SCP2 domain [14]. The binding cavity of the SCP2 domain is physically connected to the catalytic domain, thus suggesting a role in the canalization of long chain aliphatic substrates to the active site.

Such a variety of cell contexts and domain architectures suggests multiple functions for SCP2. In the last decade we have witnessed significant advances in the structural characterization of SCP2 domains from many different cells and organisms. Also, the significance of the multidomain organization of extant proteins became widely recognized [15]. Thus, it seems opportune time to review the structure-function relationship of SCP2 with a general perspective across all branches of life. The main focus of this review will be on the structural aspects of SCP2. Excellent reviews on the physiology, biochemistry, cellular biology, and molecular evolution of SCP2 are available [16–23].

2. The SCP2 superfamily of proteins

According to Pfam [24], the SCP2 superfamily includes sequences from four families: SCP2 (PF02036), SCP2_2 (PF13530), Alkyl_sulf_C (PF14864), and MDMPI_C (PF07398). Each one has a distinct Hidden Markov Model (HMM) sequence profile [25]. The SCP2 family is the most numerous and diverse, including stand-alone SCP2 domains and different multi domain proteins. The second most numerous family, SCP2_2, includes multidomain proteins, mostly associated with bacterial acetyl transferases. The third, Alkyl_sulf_C is a SCP2 domain present in bacterial alkyl sulfatases, alone or associated with a metallo-beta-lactamase domains. Finally, the MDMPI_C domain is found at the C-terminus of the mycothiol maleylpyruvate isomerase enzyme MDMPI. However, whether MDMPI_C domain can be considered an SCP2 domain is doubtful, since the only structure reported for mycothiol maleylpyruvate isomerase exhibits partial similarity to the SCP2 fold but lacks some of its typical secondary structure elements [26].

The extant SCP2 sequences includes circa 17,000 members cataloged in InterPro (http://www.ebi.ac.uk/interpro/; [27]) as the 'SCP2 sterol-binding' domain (IPR003033). For this domain, InterPro lists stand-alone proteins and multidomain proteins formed by 203 combinations of SCP2 domains with 114 different well-characterized domains.

Over 80% of the SCP2 sequences are from Bacteria. Among the most populated proteins in this group are: Eis acetyltransferase, alkyl sulfatase, stand-alone SCP2 or repeats thereof, transcriptional regulator, HxlR family, putative short-chain dehydrogenase, mycothiol maleylpyruvate isomerase, flavodoxin reductase family 1, protein kinase UbiB, alpha/beta hydrolase, cupin, 4Fe—4S ferredoxin, flavin reductase, and 3-phosphoglycerate dehydrogenase.

In Archaea, conspicuous SCP2 containing proteins are: Eis acetyltransferase, alkyl sulfatase, and stand-alone or tandem SCP2 proteins.

Among Eukaryota, typical SCP2 multidomain proteins are: hydroxysteroid dehydrogenase-like protein 2, peroxisomal multifunctional enzyme type 2, stomatin-like protein 1, bifunctional hydroxyacyl-CoA dehydrogenase/enoyl-CoA hydratase, major sperm protein, thiolase, alkyl sulfatase, nitrite/sulfite reductase ferredoxin-like, abc transporter, podocan, centrosomal protein isoform x3 protein, DHB4, protein CBR-UNC-24, estradiol 17 beta-dehydrogenase, protein serine/threonine phosphatase 2C. Also, eukaryotic cells contain single-domain SCP2 proteins, an architecture that is, with few exceptions, the most observed in plants.

The definition of SCP2 domains is based in the current set of sequence profiles in the data banks. Profiles relate sequence peculiarities to specific folds. Thus, additional SCP2 domains might be discovered examining the folds of solved structures. To that end, we searched the RCS PDB [28] using 3-D pattern recognitions algorithms (http://ekhidna.biocenter.helsinki.fi/dali_server/; [29]) and found only one SCP2 domain that scores negative with the current set of sequence profiles. It is MycE methyltransferase, a two-domain bacterial enzyme that catalyzes the *O*-methylation of sugars [30]. Since this SCP2 domain possesses no sequence similarity to the those already included in the SCP2 families, it may be used to build a new sequence profile and identify new SCP2 domains with unknown structures. The UniProt ID (http://www.uniprot.org/) and proposed names of the SCP2 domains analyzed in this review are listed in Table 1. Since abbreviated names given by different authors to SCP2 domains could be very confusing, in the text the domains are referred to by UniProt ID.

3. The structure of SCP2 domains

Several SCP2 domains from all branches of life have been characterized so far with atomic detail. A catalog of selected structures is shown in Table 2. Not included in this catalog are incomplete, highly-decorated or severely distorted versions of the SCP2 fold that presumably are unrelated to the basic domain (for instance: Pfam entries LytR_cpsA_psr and Protein of Unknown Function DUF3197; or SCOP entry SCP2-like mycothiol-dependent maleylpyruvate isomerase [31]).

SCP2 fold pertains to the $\alpha + \beta$ class of protein domains. The overall shape of the domain is dome-like, with a five-stranded β sheet as the floor and four α-helical elements forming the walls and roof. It comprises two layers of secondary structure and a connection loop (Fig. 1). Within the $\alpha + \beta$ class, SCOP database 1.75 defined the fold as: alpha-beta(3)-*X*-beta-alpha(2)-beta-alpha (2 layers: a/b, crossover loop *X* makes the third layer; antiparallel beta-sheet of five strands; order: 32145).

The fold design is remarkable in several ways. The five-stranded β sheet is bipartite, comprising one three-stranded antiparallel element from the N-terminus and one two-stranded element from the C-terminus. The arrangement of the resulting β sheet forces the whole main chain to an entropically expensive detour to arrive to the final native fold, including a long crossover loop connecting parallel strand *S*3 and *S*4. Finally, the arrangement of elements in the α-helical layer allows for the formation of the walls and roof of the dome-like structure and of a circular opening on the top, which is the main entry to the internal cavity that may serve as lipid binding site.

Twenty two superposed SCP2 structures (Table 2) are shown in Fig. 2. In spite that these structures sample all major branches of life, the superposition indicates a remarkable persistence of the secondary structural elements and their mutual spatial orientation. The structural conservation can also be appreciated by the plot of RMSD vs fraction of superposed residues (Fig. 2B); it can be seen that a group of bacterial SCP2 is the more deviant, but some SCP2 from Bacteria and Archaea cluster with yeast, insect, and mammal SCP2.

4. Sequence determinants of the SCP2 fold

SCP2 sequences of the twenty two superposed structures were manually aligned based upon structural equivalence (Fig. 3). Residues were considered structurally equivalent if they had similar space location, backbone torsion angles, and side-chain orientation. Most, but not all, residues could be unambiguously assigned; those that could not were located arbitrarily in the proximity of the aligned ones. The alignment highlights the conservation of the secondary structure elements. It can be seen that helix 1 bends 45° resulting in two segments, *H1a* and *H1b* (Fig. 1) in mammal, yeast, archaea and some bacterial SCP2. Notably, *H1b* is absent in insect and most bacterial SCP2. On another hand, *H4* alignment must be considered tentative, for this segment adopts very different orientations (see Fig. 2). The remaining elements of secondary structure are very well conserved among all the analyzed SCP2.

Table 1
UniProt ID and recommended and alternative parent protein names of the main SCP2 domains discussed in this review.

UniProt ID	Res.	Species	Protein names
DHB4_HUMAN	628–731	*Homo sapiens*	Peroxisomal multifunctional enzyme type 2; MFE-2; beta-hydroxysteroid dehydrogenase 4; 17-beta-HSD 4 D-bifunctional protein; DBP Multifunctional protein 2.
NLTP_HUMAN	433–543	*Homo sapiens*	Non-specific lipid-transfer protein; NSL-TP; Propanoyl-CoA C-acyltransferase; SCP-chi SCPX Sterol carrier protein 2; SCP-2 Sterol carrier protein X; SCP-X.
NLTP_RABIT	433–543	*Oryctolagus cuniculus*	Non-specific lipid-transfer protein; NSL-TP; Propanoyl-CoA C-acyltransferase; SCP-chi SCPX Sterol carrier protein 2; SCP-2 Sterol carrier protein X; SCP-X.
K7NSY9_HELAM	423–519	*Helicoverpa armigera*	Sterol carrier protein 2/3-oxoacyl-CoA thiolase
Q0GY13_AEDAE	1–105	*Aedes aegypti*	Sterol carrier protein 2-like 2
Q16LC3_AEDAE	1–120	*Aedes aegypti*	AAEL012704-PA
Q86PR3_AEDAE	1–110	*Aedes aegypti*	Sterol carrier protein 2
SCP2_YARLI	1–129	*Yarrowia lipolytica*	Fatty acid-binding protein; Sterol carrier protein 2; YLSCP2.
O28738_ARCFU	1–116	*Archaeoglobus fulgidus*	unspecified; uncharacterized protein
Q5SL92_THET	1–130	*Thermus thermophilus*	unspecified; uncharacterized protein
A0QY29_MYCS2	297–402	*Mycobacterium smegmatis*	Enhanced intracellular survival protein; Eis.
EIS_MYCTU	299–402	*Mycobacterium tuberculosis*	Enhanced intracellular survival protein; Eis.
D2PVF8_KRIFD	282–389	*Kribbella flavida*	GCN5-related *N*-acetyltransferase
Q3M362_ANAVT	290–395	*Anabaena variabilis*	GCN5-related *N*-acetyltransferase
Q6HXD7_BACAN	285–390	*Bacillus anthracis*	Acetyltransferase
Q831Y9_ENTFA	286–397	*Enterococcus faecalis*	unspecified; uncharacterized protein
Q9I5I9_PSEAE	538–655	*Pseudomonas aeruginosa*	SDS hydrolase SdsA1
F8KAY7_9PSED	547–660	*Pseudomonas* sp.	Sec-alkylsulfatase
F2WP51_9PSED	548–674	*Pseudomonas* sp.	PSdsA
YJCS_ECOLI	543–661	*Escherichia coli*	Putative alkyl/aryl-sulfatase YjcS
MYCE_MICGR	6–164	*Micromonospora griseorubida*	Mycinamicin VI 2′-*O*-methyltransferase; Mycinamicin biosynthesis protein E.
NLTP_BOVIN	429–539	*Bos taurus*	Non-specific lipid-transfer protein; NSL-TP; Propanoyl-CoA C-acyltransferase; SCP-chi; SCPX; Sterol carrier protein 2; SCP-2 Sterol carrier protein X; SCP-X.
NLTP_RAT	433–543	*Rattus norvegicus*	Non-specific lipid-transfer protein; NSL-TP; Propanoyl-CoA C-acyltransferase; SCP-chi; SCPX; Sterol carrier protein 2; SCP-2 Sterol carrier protein X; SCP-X.
B0FSK0_TOXGO	352–444 521–619	*Toxoplasma gondii*	D-bifunctional protein

A closer examination of the aligned structures allowed identification of a subset of thirteen residues playing a structural core role in all SCP2 structures. The identification was achieved by counting the non local number of intramolecular contacts established by the side chains (the search parameters were a distance of 4.5 Å or less and a number of contacts greater than ten). Equivalent residues that fulfill these requirements in most of the structures are marked with an asterisk in the alignment of Fig. 3. These thirteen residues concentrate a large number of long-range stabilizing contacts and can be considered a basic framework for the whole SCP2 structure. Their location in the structure is shown with an example in Fig. 4.

Once identified the structural core positions, it was trivial to locate their cognates in conventional sequence alignments. Thus, all the sequences listed in Pfam as SCP2 entries plus the MycE methyltransferase group identified in this work as pertaining to the SCP2 fold (2469 sequences) were statistically analyzed (Fig. 4, *lower panel*). Remarkably, in most cases, the structural core positions are occupied only by two or three of a reduced subset of residues: W, F, L, V, I, and M. These highly frequent residues are of a bulky hydrophobic character.

The interactions established by the structural core residues dock the α-helices at optimal distance from the inner face of the SCP2 β-sheet, and hence determine the amplitude of the putative binding cavity. Interestingly, core residues 68 and 88 (Fig. 3) dock in place the N-terminal part of helix *H4*, even in the cases where this helix partially unfolds and extends away from the core to mediate specific protein-protein interactions (see Section 7).

In addition to the above described global structure determinants, there are other very interesting local sequence-determining features conserved among SCP2 domains. The first is a subrogation of main-chain β-strand atoms by a side chain from a residue far in sequence. This is a trick used some times by proteins to fix geometrical inconsistencies in β-strand pairing. In this case, the parallel pairing of hydrogen bonds between β-strands *S1* and *S4*, which differ in length and tend to diverge under the imposition of the overall fold (Fig. 5), is completed

Table 2
A structural catalog of SCP2 domains.

UniProt entry[a]	Residues	ID[b]	Pfam[c]	Taxonomy	Organization[d]	Ligand[e]
DHB4_HUMAN	628–731	1ikt[f]	SCP2	Eukaryota	○○●	OXN
NLTP_HUMAN	433–543	2c0l[g]	SCP2	Eukaryota	○●	–
NLTP_RABIT	433–543	1c44[h]	SCP2	Eukaryota	○●	–
K7NSY9_HELAM	423–519	4uei[i]	SCP2	Eukaryota	○○●	–
Q0GY13_AEDAE	1–105	2qzt[j]	SCP2	Eukaryota	●	PLM
Q16LC3_AEDAE	1–120	3bkr[k]	SCP2	Eukaryota	●	PLM
Q86PR3_AEDAE	1–110	1pz4[l]	SCP2	Eukaryota	●	PLM
SCP2_YARLI	1–129	4jgx[m]	SCP2	Eukaryota	●	PLM
O28738_ARCFU	1–116	3cnu	SCP2	Archaea	●	–
Q5SL92_THET	1–130	2cx7[n]	SCP2	Bacteria	●	–
A0QY29_MYCS2	297–402	3sxn[o]	SCP2_2	Bacteria	○○●	–
EIS_MYCTU	299–402	3r1k[p]	SCP2_2	Bacteria	○○●	–
D2PVF8_KRIFD	282–389	4my0	SCP2_2	Bacteria	○○●	–
Q3M362_ANAVT	290–395	2ozg	SCP2_2	Bacteria	○○●	–
Q6HXD7_BACAN	285–390	3n7z[q]	SCP2_2	Bacteria	○○●	–
Q831Y9_ENTFA	300–402	2i00	SCP2_2	Bacteria	○○●	–
Q836T6_ENTFA	286–397	2hv2	SCP2_2	Bacteria	○○●	–
Q9I5I9_PSEAE	538–655	2cfu[r]	Alkyl_sulf_C	Bacteria	○○●	PEG
F8KAY7_9PSED	547–660	2yhe[s]	Alkyl_sulf_C	Bacteria	○○●	–
F2WP51_9PSED	548–674	4nur	Alkyl_sulf_C	Bacteria	○○●	–
YJCS_ECOLI	543–661	4pdx[t]	Alkyl_sulf_C	Bacteria	○○●	–
MYCE_MICGR	6–164	3sso[u]	–	Bacteria	●○	–

[a]http://www.uniprot.org/. [b]Entries in the RCS PDBank (http://www.rcsb.org/) selected as the most representative for each sequence and analyzed in this work. [c] http://pfam.xfam.org/. [d]The SCP2 domain can be a stand-alone domain or be part of a multidomain protein. The overall organization of the domains along the chain is illustrated by circles and the SCP2 domain is indicated as a black circles. The assignment was mostly based in InterPro annotations (http://www.ebi.ac.uk/interpro/). [e]Reported ligand in the crystallographic structure: OXN, Triton X–100; PLM, palmitic acid; PEG, polyethylene glycol. [f] [58]. [g] [39]. [h] [59]. [i] [56]. [j] [60]. [k] [61]. [l] [38]. [m] [34]. [n] [62]. [o] [10]. [p] [11]. [q] [12]. [r] [14]. [s] [63]. [t] [64]. [u] [30].

by a side-chain oxygen at position 117 hydrogen bound to a main-chain *N* at position 67 (thereafter the sequence numbering will be that of Fig. 3). Judging from conventional alignments, an equivalent hydrogen bond should be present in most Eukarya and Archaea SCP2 domains. In Bacteria, this feature is still present but less prevalent, and alternative solutions to the β-strand gap closure problem are more common (for instance, β-strand *S4* is two residue shorter and the hydrogen bond acceptor is located at position 119).

The second sequence-determining feature is a helical hairpin (alpha-loop-alpha) connecting antiparallel β-strands *S4* and *S5* (see Fig. 1), which are part of a β-hairpin, a motif that typically is connected by a β-turn or a short loop. Here, the connection is a much more elaborated nested hairpin of two short antiparalell α-helices (*H2* and *H3*). The loop between the two helices is very demanding in terms of sequence specificity. To ensure a 180° reversal of the backbone direction in a confined space, *H2* is C-capped with a Schellmann motif [32], which is a specific six-residue sequence of dihedral angles used in many proteins to build antiparallel α-helices. One of those φ,ψ dihedral angles is located in the upper right quadrant of the Ramachandran plot, which strongly favors residue Gly. As a consequence Gly is present at position 133 in more than 70% of all SCP2 sequences.

The third instance of a structure-determined sequence feature is the sharp 90° change in backbone direction that takes place between *H3* and *S5*. It involves only one residue, at position 144, which must adopt positive φ,ψ values in the *Ramachandran Plot* and therefore it strongly favors Gly. Indeed, more than 90% of SCP2 and Alkyl_sulf_C families have a Gly residue at position 144. In the SCP2_2 family, this residue is significantly less prevalent.

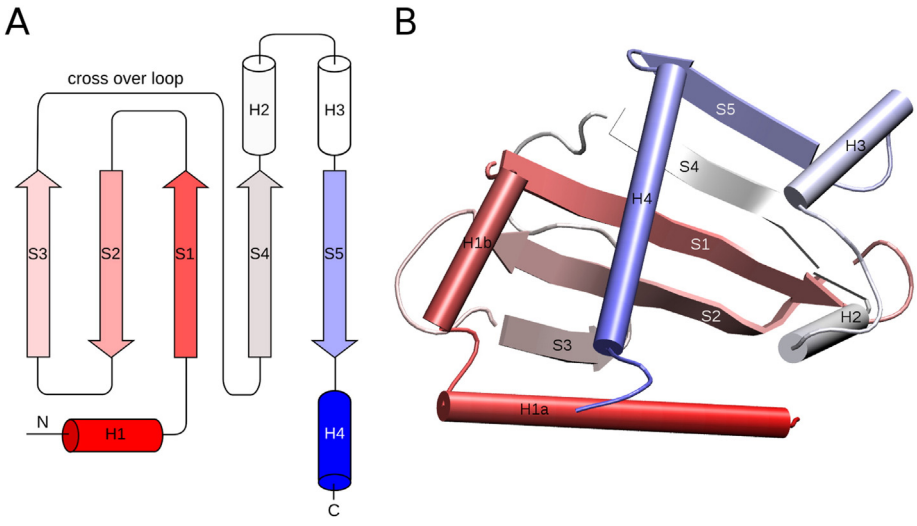

Fig. 1. SCP2 fold description. *Panel A*, secondary structure layout. *Panel B*, cartoon representation of an actual SCP2 fold (RCS PDB ID: 1ikt). Coloring is an atom-index based gradient (N-terminal red, middle with, C-terminal blue). β strands and α-helices are labeled *S1—S5* and *H1—H4*, respectively. *H1* in *Panel A* corresponds to *H1a* and *H1b* in *Panel B*, to highlight that in some members of the SCP2 family a single N-terminal helix is observed. (For interpretation of the references to color in this figure legend, the reader is referred to the web version of this article.)

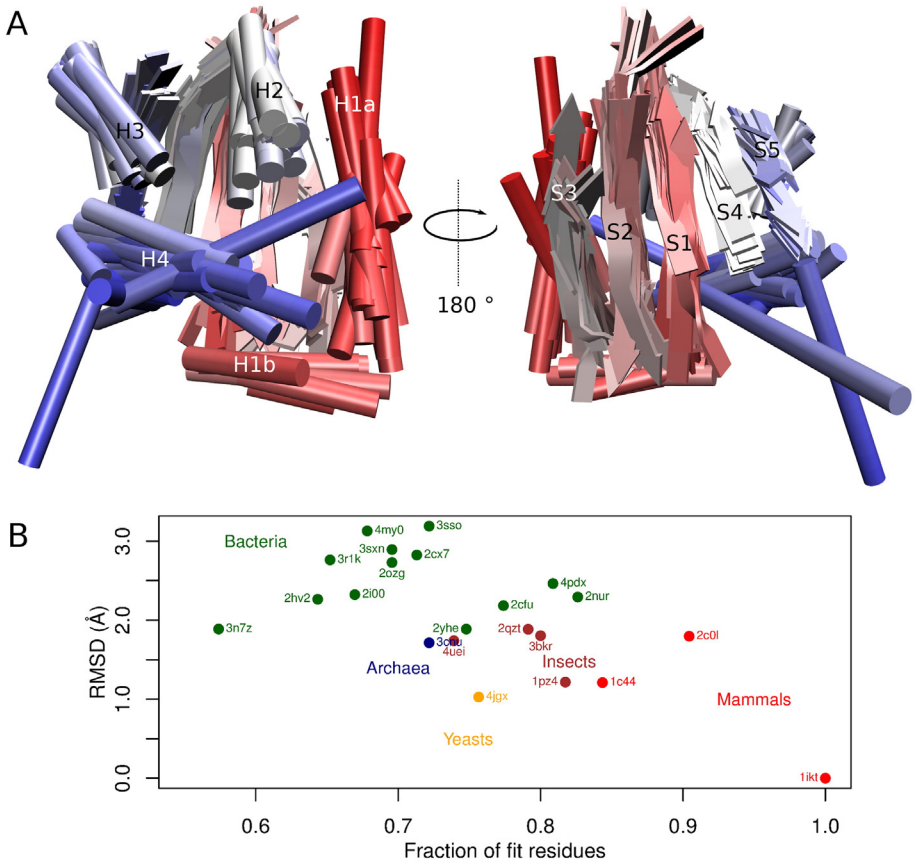

Fig. 2. Superposition of SCP2 structures. In the upper panel, superposed structures of 22 SCP2 domains (Table 2) are shown in two views related by a 180° rotation. A *Cartoon* representation was chosen to highlight the common conserved elements of secondary structure (*H*, helix; *S*, beta strand). Connecting loops were omitted for clarity. The coloring scheme allows to appreciate the location along the chain of the represented elements: red–white–blue gradient corresponds to N–terminal to C–terminal proximity. In the lower panel, the RMSD of the superposed structures are plotted as a function of the fraction of residues aligned. Only the structurally equivalent backbone atoms resulting from the superposition were used to calculate RMSD, and all the structures were superposed to the mammalian SCP2 domain of peroxisomal multifunctional enzyme type 2 (RCS PDB ID: 1ikt). (For interpretation of the references to color in this figure legend, the reader is referred to the web version of this article.)

Finally, at position 151 in the structural alignment of SCP2 and Alkyl_sulf_C families there is, almost invariably, a Gly residue. Position 151 is simultaneously the end of *S5* and the N-cap of *H4*. Such abrupt transition between different elements of secondary structure is done without displacing *H4* away from the protein core. A solution to this constraint is to force the residue at position 151 to adopt a positive φ dihedral angle. In doing that, a residue bulkier than Gly would clash with strand *S5*, explaining the strong conservation of Gly. In the SCP2_2 family (bacterial *N*-acetyl transferases) position 151 is much more variable, because the constraint is solved by making *S5* shorter and thus avoiding the internal clash. In MycE methyltransferase, which is probably a member of a new SCP2 family (see above), the conformational conflict is solved by the insertion of several residues between *S5* and *H4*.

A general conclusion may be drawn from the above analysis of the structure-determined sequence features of the SCP2 fold. The degree of conservation of sequence determined details among SCP2 and Alkyl_sulf_C families argues in favor of a common evolutionary origin. Instead, the SCP2_2 and MycE methyltransferase SCP2 families seem to have arisen from independent ancestral sequences.

5. The central binding cavity

The most important and interesting three-dimensional feature of SCP2 domains is the large internal cavity present in many of them. As mentioned above, the cavity has a floor formed by the internal side of the β–sheet and walls formed by the four α–helices. The volume of the cavity for the 22 structures listed in Table 2 was calculated using CASTp [33] and according to Ref. [34] (Table 3). In twelve structures there are cavities large enough to accommodate bulky hydrophobic ligands (>200 Å^3).

Human peroxisomal multifunctional enzyme type 2 exhibits one of the largest binding sites (over 1000 Å^3; Fig. 6, *Panel A*), and its cavity is occupied by a molecule of Triton X–100 –a detergent employed in the crystallization. This enzyme is a three-domain peroxisomal protein, with the SCP2 domain at the C-terminus. Closely related peroxisomal 3-oxoacyl-CoA thiolases have a dissimilar cavity pattern: rabbit and human thiolases posses no cavity (NLTP_HUMAN, 2c0l) and (NLTP_RABIT, 1c44; 280 Å^3; Fig. 6, *Panel B*) possesses a small one. In neither of these two structures adventitious ligands were present. On the other hand, insect peroxisomal 2/3-oxoacyl-CoA thiolase (K7NSY9_HELAM; 4uei; Fig. 6, *Panel C*) exhibits an unoccupied binding site of 320 Å^3.

The three lone SCP2 domains from insects (Fig. 6, panels *D*, *E*, and *F*) exhibit large cavities (560—1120 Å^3) and a variety of shapes and ligand binding habits. In these three proteins there is bound endogenous palmitic acid with variate stoichiometry, up to two fatty acid molecules per monomer in SCP2-like 2 (Q0GY13_AEDAE).

Yeast SCP2 (SCP2_YARLI) possesses a large cavity of over 800 Å^3 (Fig. 6, *Panel G*) with one molecule of bound palmitic acid. The ligand was purposely included in the crystallization liquor to displace natural ligands that may have been captured in the *Escherichia coli* expression cells [34].

There is only one SCP2 from Archaea with a solved three dimensional structure (O28738_ARCFU; Fig. 6, *Panel H*). The cavity of this protein is wide open due to a 90° rigid body movement of the C-terminal helix and has 376 Å^3. The cavity appears empty in the refined model, except for four water molecules.

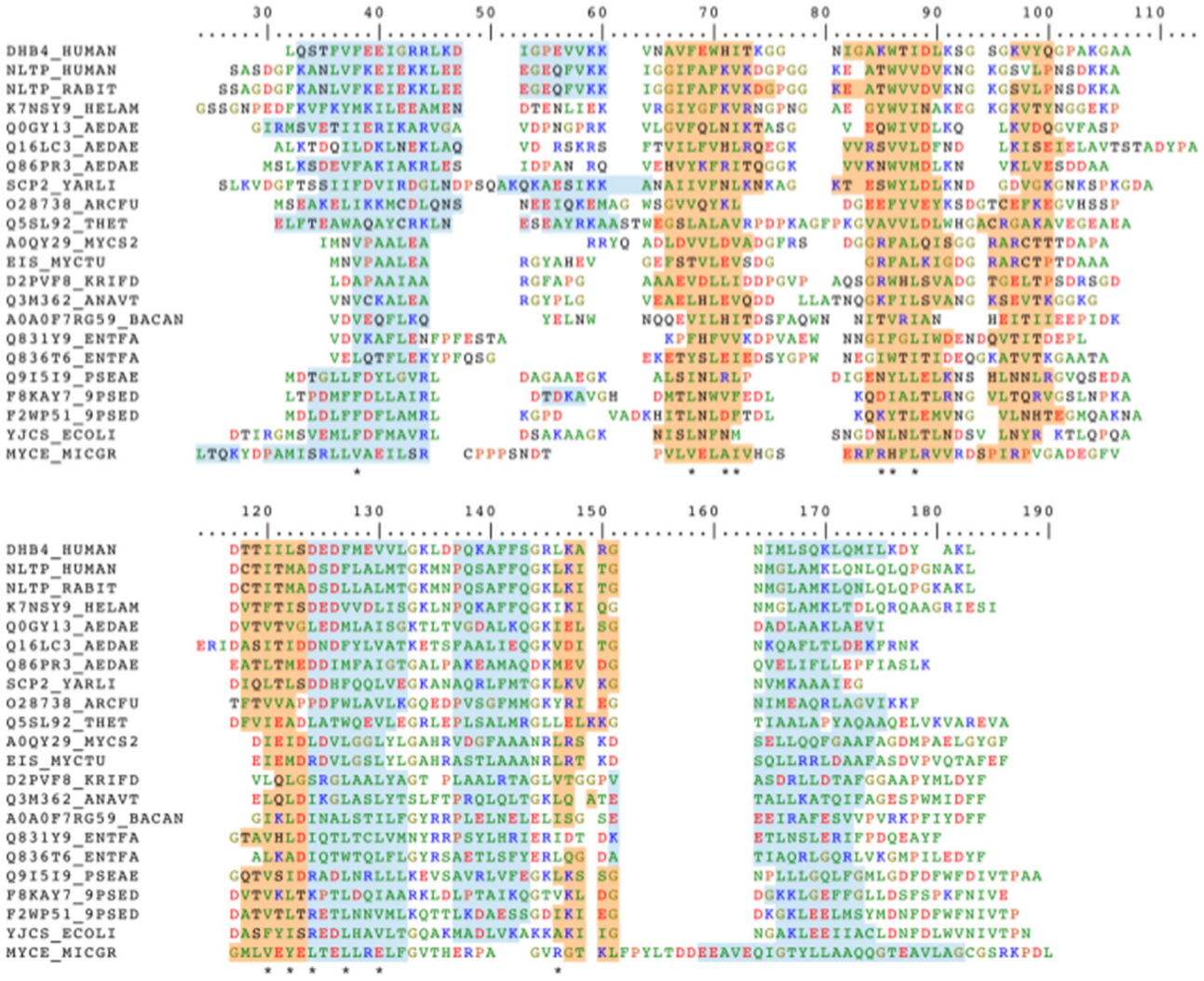

Fig. 3. Structure-guided alignment of SCP2 sequences. The sequences of the structures listed in Table 2 and superposed in Fig. 2 were aligned by hand, following a structural criteria of equivalence: spatial proximity, and similarity in backbone torsion angles and side chain orientations. α-helix and β strand segments are shown on a light blue and orange background, respectively. Simple structure calculations allowed to identify a set of residues that consistently participate in a large number of non-local inter atomic contacts through their side chains (see Section 4). The positions of these residues are marked by asterisks at the bottom of the alignment. Numbering is arbitrary.

The only solved structure of the Pfam SCP2 family in bacteria is the stand-alone domain of *Thermus thermophilus* SCP2. Its 623 Å^3 binding cavity appears empty, except for two water molecules (Q5SL92_THET; Fig. 6, *Panel I*).

The last three structures with significant cavities (259—566 Å^3) are multidomain bacterial sulfatases belonging to the Alkyl_sulf_C Pfam family: SDS hydrolase SdsA1 from *Pseudomonas aeruginosa*, (Q9I5I9_PSEAE); PSdsA from *Pseudomonas* sp. S9, (F2WP51_9PSED); Putative alkyl/aryl-sulfatase YjcS, from *Escherichia coli* (strain K12) (YJCS_ECOLI). Their cavities are shown in (Fig. 6, panels *J–L*). In SdsA1, two molecules of PEG taken from the crystallization milieu occupy the cavity. In PSdsA, part of the cavity opens to the exterior and is filled with an unusually high number of water molecules. In YjcS the cavity contains two water molecules.

The wealth of structural information on the binding site of SCP2 offers the opportunity of deepening on the analysis. The binding cavity is very variable in size and shape among the twelve structures showed in Fig. 6. The absence of a suitable cavity in the other ten included in Table 3 brings into question if having a binding site for large hydrophobic ligands is a general feature of the SCP2 superfamily. Since neither of the eight structures from SCP2_2 (PF13530) nor the structure of MycE methyltransferase (Table 3, MYCE_MICGR, 3sso) exhibits a cavity, it seems reasonable to conclude that only the SCP2 (PF02036) and Alkyl_sulf_C (PF14864) families are genuine lipid binding proteins. This reinforces the idea that SCP2_2 and MycE methyltransferase have a distinct evolutionary origin, as suggested by other structural peculiarities.

Another general aspect of SCP2 binding site regards the variability in size, shape, and openings. It can be seen in Fig. 6 that the putative void extends in two directions, sandwiched between the β-sheet and helix layers. One is parallel to the strands directions, the second is across them. At the end of each direction, the cavity connects with the outer surface, offering four potential portals for ligand entry. These features are fully illustrated by the structure of SCP2-like 2 (Fig. 6, *Panel D*), in which two perpendicular lipid molecules are located with the two polar heads pointing to two entries and their tails pointing to two opposite potential entries. These ligand binding geometries are partially represented in several other structures.

In the structures of the SCP2 (PF02036) family the openings are typical mouths (i. e., relatively small oval orifices; Fig. 7 *Panel A*). Whereas in the structures from Alkyl_sulf_C (PF14864), the openings coalesce forming a cleft (Fig. 7 *Panel B*). In both SCP2 families, openings are defined by contacts between the helical hairpin and helix *H4* or between helix *H1* and helix *H4*.

The variability of binding sites size, shape and ligand occupation suggests that an expandable cavity evolved to fit different ligands and

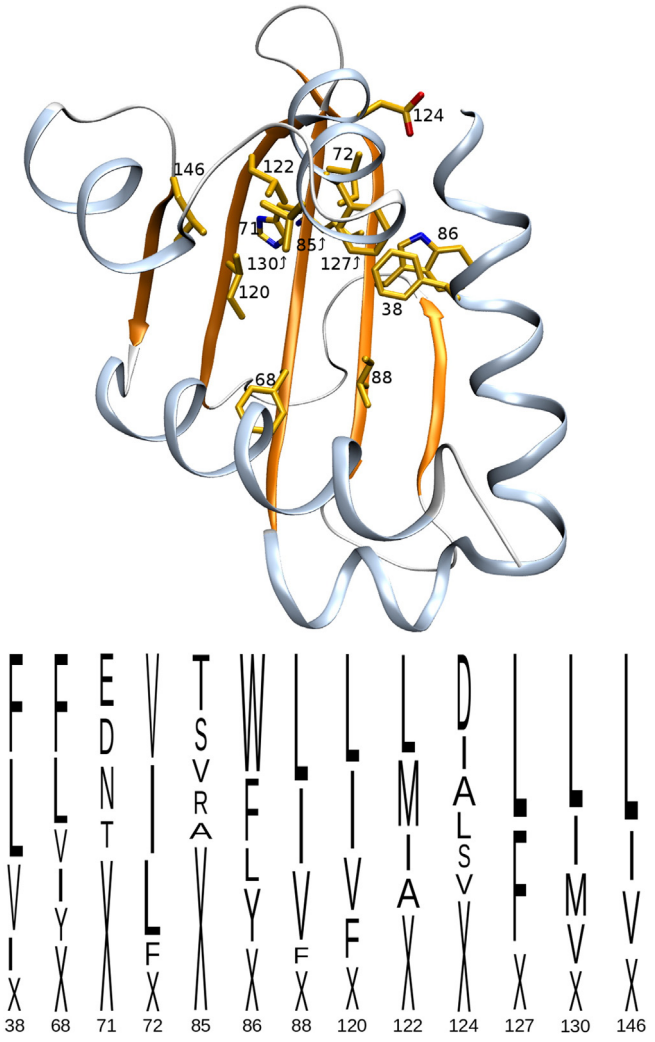

Fig. 4. The structural core residues of SCP2. In the upper panel, the SCP2 domain of human 17-beta-hydroxysteroid dehydrogenase 4 (DHB4_HUMAN, 1ikt; Table 2) was chosen to illustrate the location of these residues. In the lower panel, the residue conservation is presented as a sequence logo, with the height of the letters proportional to the prevalence at each position. The less prevalent residues were grouped and identified with *X*. The numbering is that of Fig. 3. The frequency of conserved residues was calculated from 2469 sequences from the four Pfam SCP2 families and from a blast search of MycE methyltransferase SCP2 domain. In these aligned sequences, the residues corresponding to the structural core residues were identified by comparison with the sequences of the structures in Table 2.

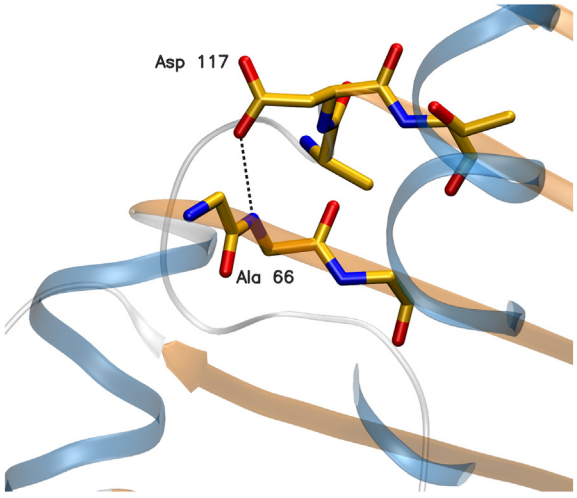

Fig. 5. The β-gap closure. In SCP2 domains β-strand *S1* is longer than β-strand *S4*, impeding a regular main-chain N → O hydrogen bonding. In most SCP2 domains, this structural defect is overcome by side-chain surrogation. As an example of this, in the structure of human 17-beta-hydroxysteroid dehydrogenase 4 SCP2 (DHB4_HUMAN, 1ikt; Table 2), Asp 117 *OD1* in β-strand *S4* establishes a strong hydrogen bond (*dashed line*) to Ala 67 *N* in (β-strand *S1*). The numbering follows the alignment in Fig. 3. To facilitate the identification of the secondary structure elements, the molecule was drawn in the same orientation than in Fig. 1. Note how nicely *CB*, *CG* and *OD1* substitute for *N*, *CO* and *O*, respectively, and fill the gap in β-strand *S4*.

binding situations. See for instance the structures of human and rabbit thiolases, which have nearly identical sequences but crystallized with no cavity (not shown) or with a minimalist and unoccupied one, respectively (Fig. 6, *Panel B*).

Inspection of the structures indicates that nearly 70% of the side-chains that limit the cavity are Leu, Ile, Val, Phe, Met or Ala residues, and Leu largely predominates among them. The total van der Waals volume occupied by these side chains is similar in all the structures, and it does not correlate with the size of the cavity (not shown).

Thus the main factor affecting the size and shape of the cavity is not the bulkiness of the side chains lining it; rather, it is a concerted breathing-like movement of the backbone what generates the changes in the volume of the internal cavity. In this movement, the β-sheet remains almost fixed, whereas concerted rigid body movements of helices *H1a*, *H2* and *H4* widen the cavity in different directions, resulting in the variety of volumes and shapes of the binding site. In addition, insect SCP2 resorts to the unwinding of helix *H1b* to make additional room for the ligands. Helix *H4* has a major role in the cavity remodeling. It behaves like a wiper on the β-sheet plane. It can be seen in Fig. 6 that the angle between helix *H4* and strand *S5* varies more than 120° (panels *C* and *H*, respectively). However, helix *H4* can also move out of the plane, or even move away from the domain body to increase the volume of the binding site.

For promiscuous ligand selection, concerted rearrangement of elements of secondary structure is better suited than redecoration of a fixed framework by side chain mutations. The strategy is compatible with the 'extended conformational selection model of ligand binding' in which ligands —in this case varying in shape or number— cause the

Table 3
Volumes of the internal cavity of SCP2 domains[a].

UniProt entry	ID	Volume (Å^3)
DHB4_HUMAN	1ikt	1101
NLTP_HUMAN	2c0l	61[b]
NLTP_RABIT	1c44	280
K7NSY9_HELAM	4uei	321
Q0GY13_AEDAE	2qzt	1127
Q16LC3_AEDAE	3bkr	775
Q86PR3_AEDAE	1pz4	562
SCP2_YARLI	4jgx	815
O28738_ARCFU	3cnu	376
Q5SL92_THET	2cx7	623
A0QY29_MYCS2	3sxn	25
EIS_MYCTU	3r1k	128
D2PVF8_KRIFD	4my0	102
Q3M362_ANAVT	2ozg	15
Q6HXD7_BACAN	3n7z	82
Q831Y9_ENTFA	2i00	57
Q836T6_ENTFA	2hv2	85
Q9I5I9_PSEAE	2cfu	547
F8KAY7_9PSED	2yhe	130
F2WP51_9PSED	4nur	566
YJCS_ECOLI	4pdx	259
MYCE_MICGR	3sso	30

[a] Volumes calculated using CASTp (http://sts.bioe.uic.edu/castp/; [33]), as described in Ref. [34]. Only protein atoms were considered to calculate the voids (i.e., ligand, water or other non protein atoms were removed from the coordinate list before volume calculation).
[b] This is an internal void isolated from the surface. There are other surface cavities close to the internal void but they are unconnected to it.

shift of an ensemble of pre-existing conformational states [35] toward those with the lower energy for binding.

6. Ligands and physicochemical basis of their interaction with SCP2

The structural information presented above can be profited in the analysis of the ligand-protein interaction. SCP2 domains form high affinity complexes with an impressive array of hydrophobic ligands: fatty acids, long chain acyl-CoAs, phospholipids, sterols, flavonoids, dyes, synthetic compounds and other lipids. Basic information about these complexes is presented in Table 4.

Although SCP2 ligands only have in common bulkiness and a hydrophobic or amphiphilic nature, they accommodate in the binding site, which is consistent with a mechanism based in soft geometrical constraints. In general, van der Waals interactions have lesser spatial restrictions than polar or hydrogen bond interactions, which have a more limited range of distances and angular approach. In line with this, the examination of the available SCP2 structures indicates that the first layer of protein heavy atoms in the limit with the internal void comprises almost invariably carbon atoms, in such a way that oxygen and nitrogen atoms are excluded from interacting with ligand atoms or occluded solvent.

A consequence of this particular nature of the SCP2 binding cavity is that there are almost no fixed water molecules inside it. In the few instances where water is observed, it is generally in the periphery of the cavity and connected to the external solvent layer. This is in contrast with the much more studied case of fatty acid-binding protein (FABP), in which the cavity —similar in volume to that of SCP2— is occupied by a significant number of well organized water molecules.

A better appreciation of the differences between FABP and SCP2 binding sites can be obtained from a comparison of *Aedes aegypti* sterol carrier protein 2-like 2 (Q0GY13_AEDAE) in complex with palmitic acid and human heart FABP in complex with oleic acid.

The binding site of heart FABP is elaborate [36], with three well-differentiated regions: (*i*) a pad of fourteen ordered and very tightly packed water molecules, held in place by a scaffold of polar and ionizable groups and packed against one edge of the carbon chain of the ligand; (*ii*) a cluster of hydrophobic side chains atoms (C—H) contacting the opposite edge of the aliphatic chain of the ligand; and (*iii*) a portal zone with polar and charged residues and water molecules holding rigidly the ligand carboxylate via hydrogen bonds and ionic interaction (Fig. 8, *Panel B*).

On the other hand, the binding site of *Aedes aegypti* SCP2-like 2 is simpler and exhibits only a hydrophobic layer of side chain atoms (C—H) that engulf the aliphatic part of the ligands and a few polar interactions (O—H, N—H) holding the polar heads in proximity to the external layer of water (Fig. 8, Panel *A*).

An analysis of the atoms interacting with the aliphatic part of the ligands further illustrates the difference between the two binding sites (Ermácora M. R., unpublished results). In heart FABP there are 3.1 van der Waals interactions (*protein* — C—H···H—C—*ligand* distances <3.2 Å) per ligand carbon atom, whereas 5.4 such interactions are found in the insect SCP2. Also, 0.7 *water* — O···H—C — *ligand* and *protein* — N/O—H···H—C — *ligand* contacts per ligand carbon atom are found in the FABP, against none and 0.12 respectively in the insect SCP2. Thus the binding site is significantly more hydrophobic and homogeneous in insect SCP2 than in FABP. The same trend is observed in the other SCP2 proteins in Table 2 that carry fatty acids in their binding sites.

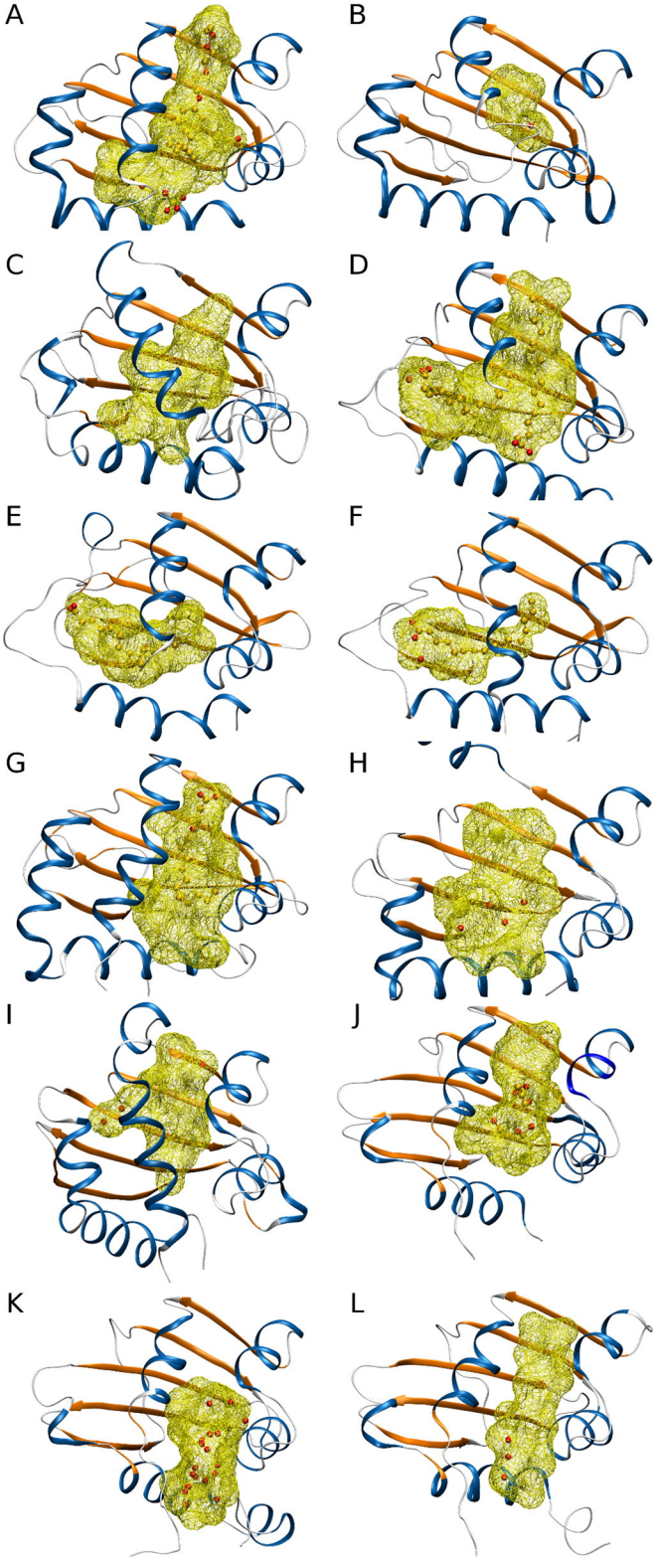

Fig. 6. Examples of SCP2 binding cavities. Twelve of the twenty two structures listed in Table 3 possess a large internal void which is, in several cases, occupied by hydrophobic ligands. (A) Human peroxisomal multifunctional enzyme type 2 (DHB4_HUMAN; 1ikt). (B) Rabbit non-specific lipid-transfer protein, peroxisomal 3-oxoacyl-CoA thiolase (NLTP_RABIT; 2c0l). (C) Insect sterol carrier protein 2/3-oxoacyl-CoA thiolase (K7NSY9_HELAM; 4uei). (D) Insect SCP2-like 2 (Q0GY13_AEDAE; 2qzt). (E) Insect SCP2-like 3 (Q16LC3_AEDAE; 3bkr). (F) Insect SCP2 (Q86PR3_AEDAE; 1pz4). (G) Yeast SCP2, Yarrowia lipolytica (SCP2_YARLI; 4jgx). (H) Archaea SCP2 (O28738_ARCFU; 3cnu). (I) Bacteria SCP2, Thermus thermophilus, (Q5SL92_THET; 2cx7). (J) SDS hydrolase SdsA1, Pseudomonas aeruginosa, (Q9I5I9_PSEAE; 2 cfu). (K) PSdsA, Pseudomonas sp. S9, (F2WP51_9PSED; 4nur). (L) Putative alkyl/aryl-sulfatase YjcS, Escherichia coli (strain K12), (YJCS_ECOLI; 4pdx). The space occupied by the cavity in each structure is delineated with a wire-frame representation. Ligands in the cavities are shown in a CPK representation, with carbon atoms in gold and oxygen in red. Water molecules are represented as pink spheres. The identity of the ligands is given in Table 2.

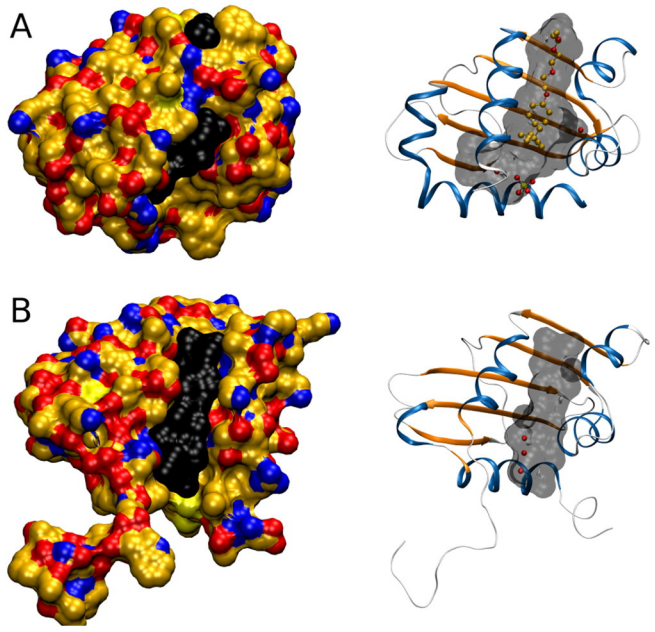

Fig. 7. Disposition and openings of the binding cavity in structures from the SCP2 and Alkyl_sulf_C Pfam families. (*A*) 17-beta-hydroxysteroid dehydrogenase 4 (DHB4_HUMAN; 1ikt; Table 2). (*B*) Putative alkyl/aryl-sulfatase YjcS (YJCS_ECOLI; 4pdx; Table 2); To visualize the openings (binding mouths and cleft), the binding cavity was filled with carbon-size, black spheres. A surface representation is shown on the left (carbon, oxygen and nitrogen atoms are in gold, red and blue, respectively). On the right, a ribbon representation illustrates the location of the binding cavity (black silhouette), and a CPK representation shows the position of the ligand, water molecules, and a phosphate anion bound to the protein surface, if applicable.

Water-water interactions are crucial for binding and participate in the mechanism and energetic of the process in multiple ways. There is an important energy term associated to the removal of a ligand from bulk solvent and also in the confinement of solvent to a limited cavity. As a result, the properties of water in a cavity are very different than in bulk solvent (see [36] and references therein). Also, when present, water must be expelled out to allow binding. On top of this, there is the problem of the energetic cost of keeping a cavity empty.

All this have generated a renewed interest in the topology and properties of water molecules in the binding site of hydrophobic compounds [36,37]. As mentioned above, the binding site of SCP2 is peculiar, for almost no water molecules can be found in it (Fig. 6). Thus, the question is if the lack of water molecules in the crystallographic structures is due to their high mobility or it reflects genuine absence. The detailed studies of the binding site of heart FABP, strongly suggest that low energy water molecules should be readily detectable in X-ray experiments. This low energy water is highly structured (ultracompact) and forms short water—water, protein—water hydrogen bonds and also *water*—O···H—C—*ligand* hydrogen bonds [36]. On the other hand, high-energy water molecules in the cavity are highly dynamic and may or may not produce enough electronic density to be refined in a X-ray structure [37].

FABP studies teach that both types of water have specific roles in the mechanisms of binding. As mentioned above, the pad of low energy water delineates the space to be occupied by the ligand and directly interacts with it. The high energy water molecules contribute to the thermodynamic of binding through the enthalpy-entropy balance and limit the length and ramification of the ligand. By comparison, the more likely explanation for the peculiarity of SCP2 binding cavity is that only high-energy water is present in it. This water goes undetected in typical X-ray experiments and thus the cavity appears empty or with extra room when occupied by a ligand. This highly mobile water should be more like that of the typical solvating water layer of proteins, in rapid exchange with bulk solvent. The displacement of this highly mobile water by a hydrophobic ligand is energetically favored because of the hydrophobic nature of the cavity. Indeed, the energetic cost of keeping high energy water in the cavity is only inferior to keep the cavity empty.

Thus, the apparent emptiness of the SCP2 binding site in some of the crystallographic structures analyzed in this review may be explained by its occupation by easily exchangeable water. However, that may not be the only reason. Indeed, experience teaches that the preparation of the apo forms of lipid binding proteins is a hard practical problem. These proteins, purified from natural sources or from heterologous recombinant expression systems, always carry bound endogenous lipids (see for instance the supplementary information for Ref. [37,38]). To prepare the apo forms harsh procedures need to be applied. Simple extractive treatments or batch delipidation with hydrophobic matrices are not always effective, and proteins must be chemically unfolded, stripped out of lipids and refolded in solvents meticulously cleaned of contaminant

Table 4
Examples of binding constants of SCP2 domains.

Ligand	SCP2 domain	K_D (μM)	Reference
NBD-stearic acid	NLTP_HUMAN	0.23[a]	[65]
RdB-stearic acid	NLTP_HUMAN	0.26[a]	[65]
cis-parinaric acid	NLTP_HUMAN	0.16–0.65[a]	[65–67]
cis-parinaric acid	YARLY_SCP2	0.08[a]	[68]
cis-parinaric acid	NLTP_HUMAN	0.36[a]	[69]
Trans-parinaric acid	NLTP_HUMAN	0.56[a]	[66]
Trans-parinaric acid	NLTP_HUMAN	0.20[a]	[69]
Pyr-lauric acid	NLTP_BOVIN	0.24[b]	[70]
Pyr-lauric acid	NLTP_RAT	~0.7[b]	[71]
Phytanic acid	NLTP_RAT	~0.9[b]	[71]
Pristanic acid	NLTP_RAT	~0.7[b]	[71]
Oleic acid	NLTP_HUMAN	0.22[c]	[72]
Linoleic acid	NLTP_HUMAN	2.06[c]	[72]
Palmitic acid	Q86PR3_AEDAE	0.35[d]	[73]
AO-palmitic acid	YARLY_SCP2	0.06[a]	[48]
cis-parinaroyl-CoA	NLTP_HUMAN	0.005[a]	[66]
Trans-parinaroyl-CoA	NLTP_HUMAN	0.003[a]	[66]
Palmitoyl-CoA	YARLY_SCP2	0.07[e]	[68]
Phytanoyl-CoA	NLTP_RAT	0.25[b]	[71]
Pristanoyl-CoA	NLTP_RAT	0.76[b]	[71]
Linoleoyl-CoA	NLTP_HUMAN	0.34; 0.95[a]	[74]
Linoleoyl-CoA	NLTP_HUMAN	0.09;1.37[f]	[74]
Cholestatrienol	NLTP_RAT	0.57[g]	[75]
Dehydroergosterol	NLTP_RAT	0.88[g]; 1.2[g]; 2.7[b]; 0.4[a]; 1.3[a]	[76,77]
Dehydroergosterol	NLTP_HUMAN	1.7[a]	[78]
Cholesterol	NLTP_HUMAN	0.3[h]; 0.03[c]	[78,72]
Cholesterol	Q86PR3_AEDAE	0.006[h]; 0.21[d]	[79,73]
Cholesterol	NLTP_RAT	2.6[b]	[71]
Pyr-cholesterol	NLTP_HUMAN	0.012[a]	[80]
NBD-cholesterol	NLTP_HUMAN	0.004[a]; 0.11[a]; 0.03[a]; 0.04[c]	[72,80,81]
NBD-cholesterol	Q86PR3_AEDAE	0.99[a]	[73]
NBD-cholesterol	B0FSK0_TOXGO	1.01[a]	[82]
β-sitosterol	Q86PR3_AEDAE	0.14[d]	[73]
Cholate	NLTP_HUMAN	144[f]	[57]
plm-pyr-pCho	NLTP_BOVIN	46[a]	[83]
NBD-PC	NLTP_HUMAN	0.11[a]	[80]
Pyr-PC	NLTP_HUMAN	0.16[a]	[80]
NBD-PC	B0FSK0_TOXGO	0.11[a]	[82]
1-O-decanyl-L-D-glucoside	NLTP_HUMAN	0.32[f]	[84]
NBD-sphingomyelin	NLTP_HUMAN	0.37[a]	[85]
Sphingomyelin	NLTP_HUMAN	0.17[a]	[85]
Ceramide	NLTP_HUMAN	0.005[a]	[85]
Glucosylceramide	NLTP_HUMAN	0.10[a]	[85]
Galactosylceramide	NLTP_HUMAN	0.11[a]	[85]
Lactosylceramide	NLTP_HUMAN	0.12[a]	[85]
Globosides	NLTP_HUMAN	0.12[a]	[85]
GM1	NLTP_HUMAN	0.043[a]	[85]
SCPI-1—SCPI-5	Q86PR3_AEDAE	0.35[a]; 0.06[a]; 0.159[a]; 0.06[a]; 0.042[a]	[86]
SCPI-1; SCPI-3	NLTP_HUMAN	3.32[d]; 6.50[d]	[53]
Curcumins analogs	Q86PR3_AEDAE	18: 12; 63, 2.3; 2.0; 0.6[d]	[87]

[a]Extrinsic fluorescence assay. [b]FRET assay. [c]SPR assay. [d]EC50%. [e]Intrinsic fluorescence assay. [f]ITC assay. [g]Light scattering assay. [h]Lipidex-1000 assay.

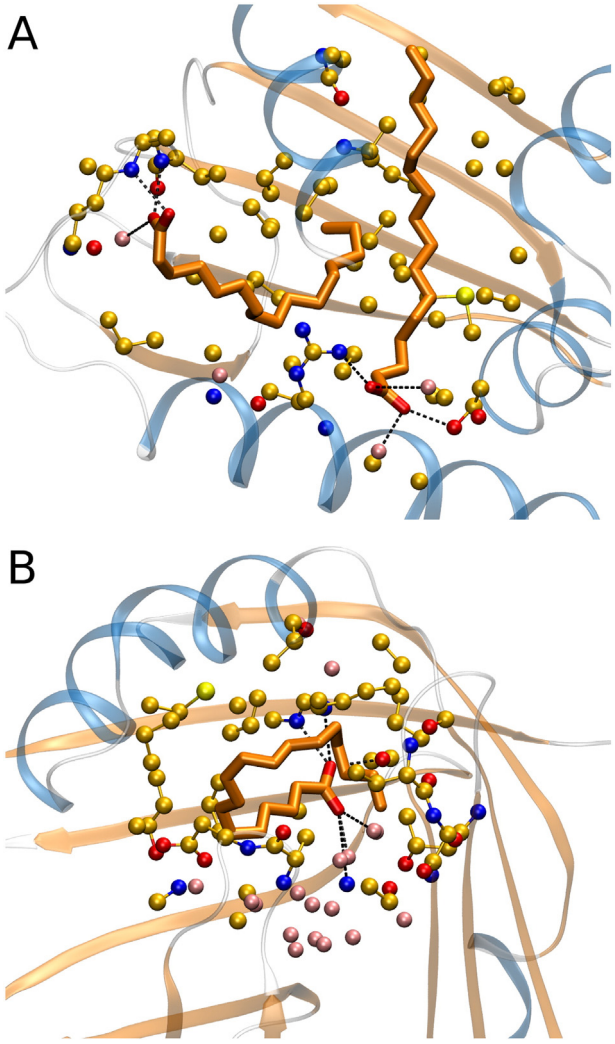

Fig. 8. Comparison between SCP2 and FABP binding sites. *Panel A*: binding site of *Aedes aegypti* sterol carrier protein 2-like 2 (Q0GY13_AEDAE; 2qzt) in complex with two molecules of palmitic acid. *Panel B*: human heart FABP (FABPH_HUMAN; 5ce4) in complex with oleic acid. Carbon atoms are shown in gold or in orange. Oxygen for water molecules was represented in pink, otherwise in red. Nitrogen and sulfur atoms are in blue and yellow respectively. Liganded fatty-acid was represented with heavy sticks.

lipids [Ermácora et al., unpublished results]. Since, none of the SCP2 structures analyzed here was reported to be from delipidated proteins, the absence of ligands in them must be taken with caution. Thus, it is likely that an additional cause of lack of electronic density in the binding site is the presence of heterogeneous or highly mobile ligands.

From the analysis of the SCP2 complexes, binding to SCP2 can be envisaged as a simple diffusion of an aliphatic chain from bulk solvent to a non-polar liquid-like phase. Once in the cavity, the ligand seems relatively free to move around and occupy different regions in it. The cavity can even allocate multiple ligands. Unlike more evolved binding sites, with defined polar interactions and rigid geometric constraints, binding to SCP2 seems to be little restrictive in terms of geometry, which offers an explanation to the broad specificity, low selectivity, and variate stoichiometry exhibited by these lipid binding proteins.

7. Specific recognition of protein sockets

An overlooked feature of SCP2 domains is that they may serve as scaffolds for a protein-protein recognition device. The C-terminal helix of SCP2 structure acts as a retractile module for homo and hetero specific interactions. This device was originally described in a typical domain of the SCP2 family, where it mediates sequence specific interactions with the peroxisome import machinery. However, during the structural analysis performed for this review, we realized that it is present in the SCP2_2 and Alkyl_sulf_C families as well, albeit with a different purpose.

Most peroxisomal matrix proteins destined to peroxisomes share the C-terminal type 1 peroxisomal targeting signal (PTS1) motif, comprising a C-terminal tripeptide with the consensus sequence -[S/A/C]-[K/H/R]-[L/M], which is specifically recognized by the C-terminal segment of the import receptor peroxin Pex5 and allows translocation of folded and functional proteins to peroxisomes [39]. The structure of Pex5 is formed by seven consecutive tetratrico peptide repeat motifs (TPR) [40]. In the case of the SCP2 domain from human non-specific lipid-transfer protein (NLTP_HUMAN), the ten C-terminal residues —upon a jack knife displacement— adopt an extended conformation, pointing away from the core and penetrating the ring-like structure of Pex5 (Fig. 9, *Panel A*). The most C-terminal *AKL* residues (141–143) of SCP2 bind within the central hole and establish specific interactions with four asparagine side chains locate on the N-terminal helices of TPR segments 4, 5, 6, and 7. This interaction is essential for the peroxisome import process and takes place with little disturbance of the core SCP2 domain. Interestingly, it takes place regardless the liganded status of the SCP2 domain [39], which allows to consider that the protein crosses the membrane not only folded but also carrying a ligand. In previous studies, it was proposed that ligand binding causes a conformational extension of the C-terminus, exposing the PTS1 motif and enabling its interaction with the receptor Pex5. This conformational change would be the basis of a 'ligand-mediated protein targeting mechanism' [41,42]. In the X-ray structure Pex5-SCP2 complex no lipid ligand was observed and the in vitro apparent affinity for a lipid ligand was roughly the same for free SCP2 and Pex5-SCP2 [39], which seems to be at odds with a 'ligand-mediated protein targeting mechanism'. However, the absence of endogenous ligands in the preparations of SCP2 and Pex5-SCP2 remains to be demonstrated (see Section 6), and thus further experiments are needed to clarify the issue.

An entirely different use for the C-terminal adapter is exemplified by the stand-alone SCP2 domain from *Archaeoglobus fulgidus* (O28738_ARCFU, 3cnu). The domain crystallizes as a homo dimer with two-fold symmetry and swapped C-terminal helices (Fig. 9, *Panel B*). Interestingly, each C-terminal helix penetrates the binding cavity of the opposite monomer, as if it were a ligand. Since very little is known on this protein other than its structure, it remains to see if its dimerization mode has a bearing on its function.

Another example of the protruding C-terminal device can be found in the SCP2_2 family, which comprises mostly bacterial acetyl transferases responsible of aminoglycoside antibiotic resistance [11]. These proteins have a complex architecture. They are hexamers (dimers of trimers), with an C3 rotation axis. Each monomer in turn possesses three domains that concertedly generate the catalytic site, one of which —the C-terminal domain— is a SCP2 domain (Fig. 9, *Panel C*). The structural meaning of the protruding C-terminal residues of the SCP domain is twofold: to latch the three domains together and to locate the general base C-terminal Phe α–carboxylate in the vicinity of the essential water molecule involved in the transfer of the Acyl-CoA moiety to the aminoglycoside amino group. Interestingly, the protruding extension of the SCP2 domain wedges between the other two domains to snuggle in place for its function.

Finally, the Alkyl_sulf_C family also exhibits a protruding C-terminus with a structural role. The overall protein belongs to the fold of metallo-β-lactamases with a conserved binuclear Zn^{2+} cluster in the active site and three domains: the N-terminal, catalytic, αββα sandwich domain; an α-helical dimerization domain; and a SCP2 C-terminal domain. Exemplified by Sec-alkylsulfatase from *Pseudomonas* sp. (F8KAY7_9PSED, 2yhe), the SCP2 domain is kept in close proximity to the other two domains by the C-terminal extension acting as a latch (Fig. 9, *Panel D*). It is tempting to speculate that the SCP2 domain acts as a receptacle for the hydrophobic alcohol released from the alkyl sulfate substrate.

It can hardly be a coincidence that the three mentioned SCP2 families include examples of C-termini that extend away from the core and connect to other domains. Thus, this plasticity of the recognition module seems a structural feature of the SCP2 fold preserved through evolution in different contexts. However, the C-termini in the different SCP2 families share no sequence homology, and convergent evolution should have recreate both the overall fold and the capacity of protrude its C-terminal residues as a interaction module. Parsimony suggests that both features must have arisen simultaneously, in which case the fold is well suited to harbor different C-terminal extensions. These considerations are of practical interest because the SCP2 fold can be envisaged as a versatile scaffold in protein engineering combining its matrix building, cargo, and interaction capacities.

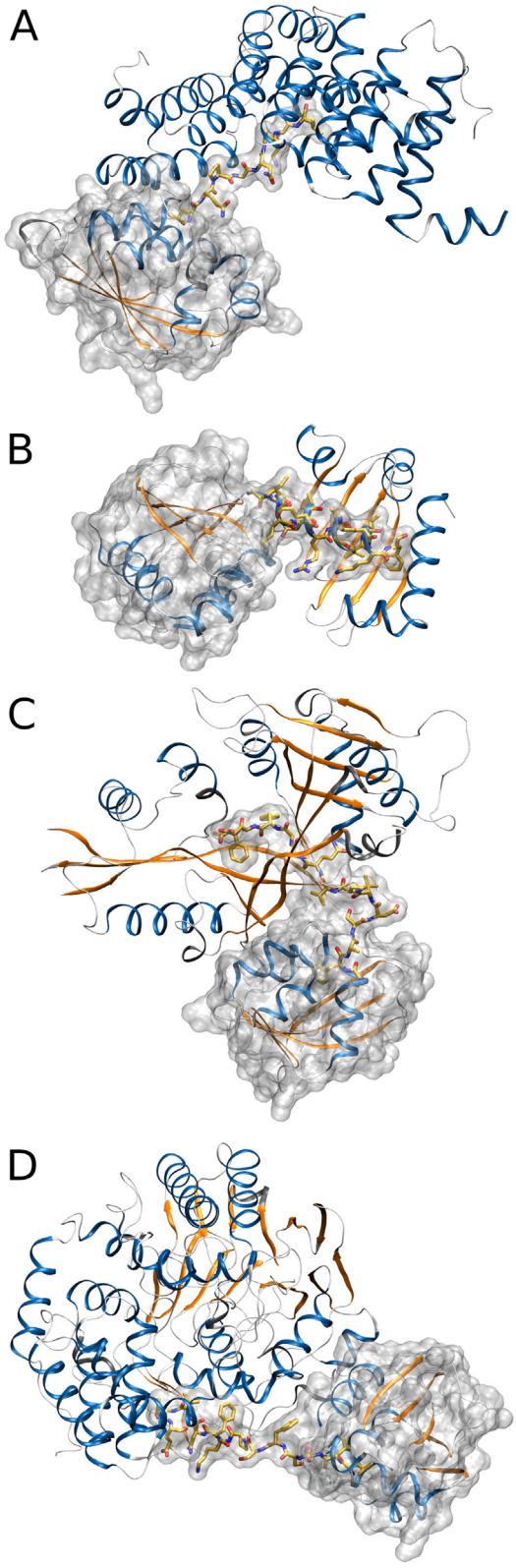

Fig. 9. The C-terminus of SCP2 domains as a recognition device. *Panel A*. The SCP2 domain of human non-specific lipid-transfer protein (NLTP_HUMAN; 2c0l; highlighted with a transparent surface) docks into the TPR domain of the import receptor peroxin Pex5 via the C-terminal ten residues (atom-colored sticks). *Panel B*. The *Archaeoglobus fulgidus* SCP2 domain (O28738_ARCFU, 3cnu) forms a homodimer with two-fold symmetry and C-terminal helices swapping. One of the monomers has been represented as a transparent surface to highlight the protrusion of the C-terminus into the binding cavity of the opposite monomer. *Panel C*. The enhanced intracellular survival protein from *Mycobacterium tuberculosis* (EIS_MYCTU, 3r1k) possesses three domains. The most C-terminal is a SCP2 domain whose last ten residues wedge into the other two domains and locate the catalytic α–carboxilate of a strictly conserved Phe residue in position for water mediated transfer of an acetyl group from Acyl-CoA to a aminoglycoside $-NH_2$ group. *Panel D*. The distal residues of the C-terminus of the SCP2 domain of Sec-alkylsulfatase from *Pseudomonas* sp. (F8KAY7_9PSED, 2yhe, transparent surface) protrude into the catalytic domain of the enzyme.

8. Interaction with membranes and lipid transfer activity

Only members of the SCP2 family have been studied in deep for its capacity to transfer lipids to membranes. It is unknown if members of the SCP2_2 or the Alkyl_sulf C families SCP-2 posses such activity. The first protein responsible for accelerating the translocation from donor to acceptor membranes of sterols. Purified in 1977 by Bloj et al. [43] from rat liver homogenates, was identified as SCP2 [6]. These initial findings were confirmed and extended by many others. The literature is too large to be fully listed here, and only a few examples are given. In vitro transfer of phospholipids between membranes is greatly accelerated by rat liver SCP2 [44]. SCP2 stimulates intermembrane sterol transfer by direct interaction with sterol in the membrane and enhancing its desorption from the membrane [45]. Also, SCP2 stimulates the exchange of glycosphingolipids and gangliosides [46], fatty acids [47,48], and oxidized derivatives [49,47].

The mechanism of SCP2-mediated transfer enhancement for yeast SCP2 was described with a collisional model [48], involving lipid binding and membrane interaction. The interaction of SCP2 with vesicles was probed by circular dichroism [48,50], rotational correlation time [51], and membrane surface pressure [52]. SCP2 membrane interaction and lipid transport depend on vesicle composition, charge, curvature and concentration, being higher for small highly-curved negatively-charge vesicles [53,54,48]. Strikingly, this feature is observed from yeast to mammals SCP2 and could be related to the fact that most SCP2 have a surface patch of positive electrostatic potential. This suggests that electrostatic interactions are important for SCP2 interaction with membranes, as it is reported for many other protein-membrane interactions [55]. The SCP2 positive patch is predominantly located at helices *H2*, *H3*, and/or *H4* (Fig. 1), were most of the SCP2 structures have openings that could be the path for ligand access and/or exit [56]. NMR relaxation experiments of human SCP2 also identified high mobility in α helices *H2*, *H3*, and *H4*, which is lost after ligand binding [57]. This conformational plasticity might be related to the access/exit of diverse lipid ligands to the binding pocket and with the optimization of protein-ligand and protein-membrane contacts.

The selectivity of the interaction may be determined by the composition and biophysical properties of the membranes, however other mechanisms are utilized as well. Interaction of SCP2 with other soluble or membrane-associated proteins may allow targeting to specific organelles. The best studied case is the import to peroxisome of human non-specific lipid-transfer protein (NLTP_HUMAN), mediated by the interaction with the receptor Pex5 (see Section 7). In the X-ray structure of the complex, the primary recognition motif is the peroxisomal targeting signal (PTS1) [39]. However, there is also a secondary interaction surface

mediated by SCP2 residues in α helices *H1b* and *H2*. The residues involved in the secondary binding site are not conserved among peroxisomal SCP2, and more structural studies, on this and other SCP2-peroxin complexes, are needed to shed more light on this issue.

9. Concluding remarks

The SCP2 fold is a very successful and widespread domain scaffold present in all forms of life. It fulfills many different roles, including modular protein matrix building, lipid binding and transfer, catalytic assistance, and protein-protein recognition. Although the discovery of SCP2 proteins can be traced back to the early 1970s, the importance of this domain is only now beginning to be fully appreciated. Structural features common to the SCP2 fold are described in this review, including the organization of its lipid-binding cavity and the logic behind the promiscuity of ligand recognition. Over two hundred of different combinations of SCP2 with more than one hundred different domains are currently known. An effort has been made to clarify the structural classification of the SCP2 domains and to bridge the gap between sequence and structure analysis. As a result, we can clearly see that most of the natural history and functional aspects related to SCP2 remain to be discovered, particularly in microorganisms and plants, where most of this domain has been found.

Ethics guidelines

The authors declare that they have no conflict of interest. This article does not contain studies with human or animal subjects performed by the authors.

Conflict of interest statement

The authors declare no competing financial interest.

Transparency document

The Transparency document associated with this article can be found, in online version.

Acknowledgements

This work was supported by grants from CONICET (PIP-GI 11220130100277CO) and the Universidad Nacional de Quilmes (PP 53/1002).

References

[1] R.K. Ockner, J.A. Manning, R.B. Poppenhausen, W.K. Ho, A binding protein for fatty acids in cytosol of intestinal mucosa, liver, myocardium, and other tissues, Science 177 (1972) 56–58.
[2] J.F. Glatz, Lipids and lipid binding proteins: a perfect match, Prostaglandins Leukot. Essent. Fat. Acids 93 (2015) 45–49.
[3] S. Lev, Non-vesicular lipid transport by lipid-transfer proteins and beyond, Nat. Rev. Mol. Cell Biol. 11 (2010) 739–750.
[4] G. D'Angelo, M. Vicinanza, M.A. De Matteis, Lipid-transfer proteins in biosynthetic pathways, Curr. Opin. Cell Biol. 20 (2008) 360–370.
[5] B. Bloj, M.E. Hughes, D.B. Wilson, D.B. Zilversmit, Isolation and amino acid analysis of a nonspecific phospholipid transfer protein from rat liver, FEBS Lett. 96 (1978) 87–89.
[6] B.J. Noland, R.E. Arebalo, E. Hansbury, T.J. Scallen, Purification and properties of sterol carrier protein 2, J. Biol. Chem. 255 (1980) 4282–4289.
[7] B.J. Poorthuis, J.F. Glatz, R. Akeroyd, K.W. Wirtz, A new high-yield procedure for the purification of the non-specific phospholipid transfer protein from rat liver, Biochim. Biophys. Acta 665 (1981) 256–261.
[8] J.M. Trzaskos, J.L. Gaylor, Cytosolic modulators of activities of microsomal enzymes of cholesterol biosynthesis. Purification and characterization of a non-specific lipid-transfer protein, Biochim. Biophys. Acta 751 (1983) 52–65.
[9] F. Liu, X. Zhang, C. Lu, X. Zeng, Y. Li, D. Fu, G. Wu, Non-specific lipid transfer proteins in plants: presenting new advances and an integrated functional analysis, J. Exp. Bot. 66 (2015) 5663–5681.
[10] K.H. Kim, D.R. An, J. Song, J.Y. Yoon, H.S. Kim, H.J. Yoon, H.N. Im, J. Kim, D.J. Kim, S.J. Lee, K. Kim, H. Lee, H. Kim, E. Jo, J.Y. Lee, S.W. Suh, Mycobacterium tuberculosis Eis protein initiates suppression of host immune responses by acetylation of DUSP16/MKP-7, Proc. Natl. Acad. Sci. U. S. A. 109 (2012) 7729–7734.
[11] W. Chen, T. Biswas, V.R. Porter, O.V. Tsodikov, S. Garneau-Tsodikova, Unusual regioversatility of acetyltransferase Eis, a cause of drug resistance in XDR-TB, Proc. Natl. Acad. Sci. U. S. A. 108 (2011) 9804–9808.
[12] K.D. Green, T. Biswas, C. Chang, R. Wu, W. Chen, B.K. Janes, D. Chalupska, P. Gornicki, P.C. Hanna, O.V. Tsodikov, A. Joachimiak, S. Garneau-Tsodikova, Biochemical and structural analysis of an Eis family aminoglycoside acetyltransferase from bacillus anthracis, Biochemistry 54 (2015) 3197–3206.
[13] M.J. Willby, K.D. Green, C.S. Gajadeera, C. Hou, O.V. Tsodikov, J.E. Posey, S. Garneau-Tsodikova, Potent inhibitors of acetyltransferase Eis overcome kanamycin resistance in *Mycobacterium tuberculosis*, ACS Chem. Biol. 11 (2016) 1639–1646.
[14] G. Hagelueken, T.M. Adams, L. Wiehlmann, U. Widow, H. Kolmar, B. Tummler, D.W. Heinz, W. Schubert, The crystal structure of SdsA1, an alkylsulfatase from *Pseudomonas aeruginosa*, defines a third class of sulfatases, Proc. Natl. Acad. Sci. U. S. A. 103 (2006) 7631–7636.
[15] D. Zhang, L.M. Iyer, A.M. Burroughs, L. Aravind, Resilience of biochemical activity in protein domains in the face of structural divergence, Curr. Opin. Struct. Biol. 26 (2014) 92–103.
[16] S.M. Pfeifer, E.E. Furth, T. Ohba, Y.J. Chang, H. Rennert, N. Sakuragi, J.T. Billheimer, J.F. Strauss III, Sterol carrier protein 2: a role in steroid hormone synthesis? J. Steroid Biochem. Mol. Biol. 47 (1993) 167–172.
[17] U. Seedorf, P. Ellinghaus, J. Roch Nofer, Sterol carrier protein-2, Biochim. Biophys. Acta 1486 (2000) 45–54.
[18] M. Bun-ya, Y. Muro, T. Niki, J. Kondo, T. Kamiryo, New aspects of sterol carrier protein 2 (nonspecific lipid-transfer protein) in fusion proteins and in peroxisomes, Cell. Biochem. Biophys. 32 (Spring 2000) 107–116.
[19] A.M. Gallegos, B.P. Atshaves, S.M. Storey, O. Starodub, A.D. Petrescu, H. Huang, A.L. McIntosh, G.G. Martin, H. Chao, A.B. Kier, F. Schroeder, Gene structure, intracellular localization, and functional roles of sterol carrier protein-2, Prog. Lipid Res. 40 (2001) 498–563.
[20] N.J. Stolowich, A.D. Petrescu, H. Huang, G.G. Martin, A.I. Scott, F. Schroeder, Sterol carrier protein-2: structure reveals function, Cell. Mol. Life Sci. 59 (2002) 193–212.
[21] K.W.A. Wirtz, Phospholipid transfer proteins in perspective, FEBS Lett. 580 (2006) 5436–5441.
[22] J. Edqvist, K. Blomqvist, Fusion and fission, the evolution of sterol carrier protein-2, J. Mol. Evol. 62 (2006) 292–306.
[23] F. Schroeder, B.P. Atshaves, A.L. McIntosh, A.M. Gallegos, S.M. Storey, R.D. Parr, J.R. Jefferson, J.M. Ball, A.B. Kier, Sterol carrier protein-2: new roles in regulating lipid rafts and signaling, Biochim. Biophys. Acta 1771 (2007) 700–718.
[24] R.D. Finn, P. Coggill, R.Y. Eberhardt, S.R. Eddy, J. Mistry, A.L. Mitchell, S.C. Potter, M. Punta, M. Qureshi, A. Sangrador-Vegas, G.A. Salazar, J. Tate, A. Bateman, The Pfam protein families database: towards a more sustainable future, Nucleic Acids Res. 44 (2016) D279–D285.
[25] R.D. Finn, J. Clements, W. Arndt, B.L. Miller, T.J. Wheeler, F. Schreiber, A. Bateman, S.R. Eddy, HMMER web server: 2015 update, Nucleic Acids Res. 43 (2015) W30–W38.
[26] R. Wang, Y. Yin, F. Wang, M. Li, J. Feng, H. Zhang, J. Zhang, S. Liu, W. Chang, Crystal structures and site-directed mutagenesis of a mycothiol-dependent enzyme reveal a novel folding and molecular basis for mycothiol-mediated maleylpyruvate isomerization, J. Biol. Chem. 282 (2007) 16288–16294.
[27] A. Mitchell, H. Chang, L. Daugherty, M. Fraser, S. Hunter, R. Lopez, C. McAnulla, C. McMenamin, G. Nuka, S. Pesseat, A. Sangrador-Vegas, M. Scheremetjew, C. Rato, S. Yong, A. Bateman, M. Punta, T.K. Attwood, C.J.A. Sigrist, N. Redaschi, C. Rivoire, I. Xenarios, D. Kahn, D. Guyot, P. Bork, I. Letunic, J. Gough, M. Oates, D. Haft, H. Huang, D.A. Natale, C.H. Wu, C. Orengo, I. Sillitoe, H. Mi, P.D. Thomas, R.D. Finn, The InterPro protein families database: the classification resource after 15 years, Nucleic Acids Res. 43 (2015) D213–D221.
[28] H.M. Berman, J. Westbrook, Z. Feng, G. Gilliland, T.N. Bhat, H. Weissig, I.N. Shindyalov, P.E. Bourne, The Protein Data Bank, Nucleic Acids Res. 28 (2000) 235–242.
[29] L. Holm, P. Rosenström, Dali server: conservation mapping in 3D, Nucleic Acids Res. 38 (2010) W545–W549.
[30] D.L. Akey, S. Li, J.R. Konwerski, L.A. Confer, S.M. Bernard, Y. Anzai, F. Kato, D.H. Sherman, J.L. Smith, A new structural form in the SAM/metal-dependent O-methyltransferase family: MycE from the mycinamicin biosynthetic pathway, J. Mol. Biol. 413 (2011) 438–450.
[31] L. Lo Conte, S.E. Brenner, T.J.P. Hubbard, C. Chothia, A.G. Murzin, SCOP database in 2002: refinements accommodate structural genomics, Nucleic Acids Res. 30 (2002) 264–267.
[32] E.J. Milner-White, Recurring loop motif in proteins that occurs in right-handed and left-handed forms. Its relationship with alpha-helices and beta-bulge loops, J. Mol. Biol. 199 (1988) 503–511.
[33] J. Dundas, Z. Ouyang, J. Tseng, A. Binkowski, Y. Turpaz, J. Liang, CASTp: computed atlas of surface topography of proteins with structural and topographical mapping of functionally annotated residues, Nucleic Acids Res. 34 (2006) W116–W118.
[34] F.P. De Berti, S. Capaldi, R. Ferreyra, N. Burgardt, J.P. Acierno, S. Klinke, H.L. Monaco, M.R. Ermácora, The crystal structure of sterol carrier protein 2 from *Yarrowia lipolytica* and the evolutionary conservation of a large, non-specific lipid-binding cavity, J. Struct. Funct. Genom. 14 (2013) 145–153.
[35] P. Csermely, R. Palotai, R. Nussinov, Induced fit, conformational selection and independent dynamic segments: an extended view of binding events, Trends Biochem. Sci. 35 (2010) 539–546.
[36] E.I. Howard, B. Guillot, M.P. Blakeley, M. Haertlein, M. Moulin, A. Mitschler, A. Cousido-Siah, F. Fadel, W.M. Valsecchi, T. Tomizaki, T. Petrova, J. Claudot, A. Podjarny, High-resolution neutron and X-ray diffraction room-temperature studies

of an H-FABP-oleic acid complex: study of the internal water cluster and ligand binding by a transferred multipolar electron-density distribution, IUCrJ 3 (2016) 115–126.
[37] S. Matsuoka, S. Sugiyama, D. Matsuoka, M. Hirose, S. Lethu, H. Ano, T. Hara, O. Ichihara, S.R. Kimura, S. Murakami, H. Ishida, E. Mizohata, T. Inoue, M. Murata, Water-mediated recognition of simple alkyl chains by heart-type fatty-acid-binding protein, Angew. Chem. Int. Ed. Eng. 54 (2015) 1508–1511.
[38] D.H. Dyer, S. Lovell, J.B. Thoden, H.M. Holden, I. Rayment, Q. Lan, The structural determination of an insect sterol carrier protein-2 with a ligand-bound C16 fatty acid at 1.35—a resolution, J. Biol. Chem. 278 (2003) 39085–39091.
[39] W.A. Stanley, F.V. Filipp, P. Kursula, N. Schuller, R. Erdmann, W. Schliebs, M. Sattler, M. Wilmanns, Recognition of a functional peroxisome type 1 target by the dynamic import receptor pex5p, Mol. Cell 24 (2006) 653–663.
[40] L.D. D'Andrea, L. Regan, TPR proteins: the versatile helix, Trends Biochem. Sci. 28 (2003) 655–662.
[41] U. Seedorf, S. Scheek, T. Engel, C. Steif, H.J. Hinz, G. Assmann, Structure-activity studies of human sterol carrier protein 2, J. Biol. Chem. 269 (1994) 2613–2618.
[42] F.L. García, T. Szyperski, J.H. Dyer, T. Choinowski, U. Seedorf, H. Hauser, K. Wüthrich, NMR structure of the sterol carrier protein-2: implications for the biological role, J. Mol. Biol. 295 (2000) 595–603.
[43] B. Bloj, D.B. Zilversmit, Rat liver proteins capable of transferring phosphatidylethanolamine. Purification and transfer activity for other phospholipids and cholesterol, J. Biol. Chem. 252 (1977) 1613–1619.
[44] A.N. Leonard, D.E. Cohen, Submicellar bile salts stimulate phosphatidylcholine transfer activity of sterol carrier protein 2, J. Lipid Res. 39 (1998) 1981–1988.
[45] J.K. Woodford, S.M. Colles, S. Myers-Payne, J.T. Billheimerb, F. Schroeder, Sterol carrier protein-2 stimulates intermembrane sterol transfer by direct membrane interaction, Chem. Phys. Lipids 76 (1995) 73–84.
[46] B. Bloj, D.B. Zilversmit, Accelerated transfer of neutral glycosphingolipids and ganglioside GM1 by a purified lipid transfer protein, J. Biol. Chem. 256 (1981) 5988–5991.
[47] L. Viitanen, M. Nylund, D.M. Eklund, C. Alm, A. Eriksson, J. Tuuf, T.A. Salminen, P. Mattjus, J. Edqvist, Characterization of SCP-2 from *Euphorbia lagascae* reveals that a single Leu/Met exchange enhances sterol transfer activity, FEBS J. 273 (2006) 5641–5655.
[48] L.J. Falomir Lockhart, N.I. Burgardt, R.G. Ferreyra, M. Ceolin, M.R. Ermácora, B. Corsico, Fatty acid transfer from *Yarrowia lipolytica* sterol carrier protein 2 to phospholipid membranes, Biophys. J. 97 (2009) 248–256.
[49] A.W. Girotti, T. Kriska, Binding and cytotoxic trafficking of cholesterol hydroperoxides by sterol carrier protein-2, in: Armstrong (Ed.), Advanced Protocols in Oxidative Stress III, Methods in Molecular Biology, vol. 1208, Springer Science+Business Media, New York 2015, pp. 421–435.
[50] H. Huang, A.M. Gallegos, M. Zhou, J.M. Ball, F. Schroeder, Role of the sterol carrier protein-2 N-terminal membrane binding domain in sterol transfer, Biochemistry 41 (2002) 12149–12162.
[51] T.W. Gadella Jr., P.I. Bastiaens, A.J. Visser, K.W. Wirtz, Shape and lipid-binding site of the nonspecific lipid-transfer protein (sterol carrier protein 2): a steady-state and time-resolved fluorescence study, Biochemistry 30 (1991) 5555–5564.
[52] A. van Amerongen, R.A. Demel, J. Westerman, K.W. Wirtz, Transfer of cholesterol and oxysterol derivatives by the nonspecific lipid transfer protein (sterol carrier protein 2): a study on its mode of action, Biochim. Biophys. Acta 1004 (1989) 36–43.
[53] H. Huang, J.M. Ball, J.T. Billheimer, F. Schroeder, Interaction of the N-terminus of sterol carrier protein 2 with membranes: role of membrane curvature, Biochem. J. 344 (1999) 593–603.
[54] G.G. Martin, H.A. Hostetler, A.L. McIntosh, S.E. Tichy, B.J. Williams, D.H. Russell, J.M. Berg, T.A. Spencer, J. Ball, A.B. Kier, F. Schroeder, Structure and function of the sterol carrier protein-2 N-terminal presequence, Biochemistry 47 (2008) 5915–5934.
[55] A. Mulgrew-Nesbitt, K. Diraviyam, J. Wang, S. Singh, P. Murray, Z. Li, L. Rogers, N. Mirkovic, D. Murray, The role of electrostatics in protein–membrane interactions, Biochim. Biophys. Acta 1761 (2006) 812–826.
[56] H. Ma, Y. Ma, X. Liu, D.H. Dyer, P. Xu, K. Liu, Q. Lan, H. Hong, J. Peng, R. Peng, NMR structure and function of *Helicoverpa armigera* sterol carrier protein-2, an important insecticidal target from the cotton bollworm, Sci. Rep. 5 (2015) 18186.
[57] F.V. Filipp, M. Sattler, Conformational plasticity of the lipid transfer protein SCP2, Biochemistry 46 (2007) 7980–7991.
[58] A.M. Haapalainen, D.M. Van Aalten, G. Meriläinen, J.E. Jalonen, P. Pirilä, R.K. Wierenga, J.K. Hiltunen, T. Glumoff, Crystal structure of the liganded SCP-2-like domain of human peroxisomal multifunctional enzyme type 2 at 1.75 Å resolution, J. Mol. Biol. 313 (2001) 1127–1138.
[59] T. Choinowski, H. Hauser, K. Piontek, Structure of sterol carrier protein 2 at 1.8 Å resolution reveals a hydrophobic tunnel suitable for lipid binding, Biochemistry 39 (2000) 1897–1902.
[60] D.H. Dyer, V. Wessely, K.T. Forest, Q. Lan, Three-dimensional structure/function analysis of SCP-2-like2 reveals differences among SCP-2 family members, J. Lipid Res. 49 (2008) 644–653.
[61] D.H. Dyer, I. Vyazunova, J.M. Lorch, K.T. Forest, Q. Lan, Characterization of the yellow fever mosquito sterol carrier protein-2 like 3 gene and ligand-bound protein structure, Mol. Cell. Biochem. 326 (2009) 67–77.
[62] A.K. Goroncy, K. Murayama, M. Shirouzu, S. Kuramitsu, T. Kigawa, S. Yokoyama, NMR and X-ray structures of the putative sterol carrier protein 2 from *Thermus thermophilus* HB8 show conformational changes, J. Struct. Funct. Genom. 11 (2010) 247–256.
[63] T. Knaus, M. Schober, B. Kepplinger, M. Faccinelli, J. Pitzer, K. Faber, P. Macheroux, U. Wagner, Structure and mechanism of an inverting alkylsulfatase from *Pseudomonas* sp. DSM6611 specific for secondary alkyl sulfates, FEBS J. 279 (2012) 4374–4384.
[64] Y. Liang, Z. Gao, Y. Dong, Q. Liu, Structural and functional analysis show that the *Escherichia coli* uncharacterized protein YjcS is likely an alkylsulfatase, Protein Sci. 23 (2014) 1442–1450.
[65] F. Schroeder, S.C. Myers-Payne, J.T. Billheimer, W.G. Wood, Probing the ligand binding sites of fatty acid and sterol carrier proteins: effects of ethanol, Biochemistry 34 (1995) 11919–11927.
[66] A. Frolov, T.H. Cho, J.T. Billheimer, F. Schroeder, Sterol carrier protein-2, a new fatty acyl coenzyme A-binding protein, J. Biol. Chem. 271 (1996) 31878–31884.
[67] N.J. Stolowich, A. Frolov, B. Atshaves, E.J. Murphy, C.A. Jolly, J.T. Billheimer, A.I. Scott, F. Schroeder, The sterol carrier protein-2 fatty acid binding site: an NMR, circular dichroic, and fluorescence spectroscopic determination, Biochemistry 36 (1997) 1719–1729.
[68] R.G. Ferreyra, N.I. Burgardt, D. Milikowski, G. Melen, A.R. Kornblihtt, E.C.D. Angelica, J.A. Santomé, M.R. Ermácora, A yeast sterol carrier protein with fatty-acid and fatty-acyl-CoA binding activity, Arch. Biochem. Biophys. 453 (2006) 197–206.
[69] F. Schroeder, A. Frolov, O. Starodub, B.B. Atshaves, W. Russell, A. Petrescu, H. Huang, A.M. Gallegos, A. McIntosh, D. Tahotna, D.H. Russell, J.T. Billheimer, C.L. Baum, A.B. Kier, Pro-sterol carrier protein-2: role of the N-terminal presequence in structure, function, and peroxisomal targeting, J. Biol. Chem. 275 (2000) 25547–25555.
[70] T.B. Dansen, J. Westerman, F.S. Wouters, R.J. Wanders, A. van Hoek, T.W.J. Gadella, K.W. Wirtz, High-affinity binding of very-long-chain fatty acyl-CoA esters to the peroxisomal non-specific lipid-transfer protein (sterol carrier protein-2), Biochem. J. 339 (1999) 193–199.
[71] U. Seedorf, M. Raabe, P. Ellinghaus, F. Kannenberg, M. Fobker, T. Engel, S. Denis, F. Wouters, K.W. Wirtz, R.J. Wanders, N. Maeda, G. Assmann, Defective peroxisomal catabolism of branched fatty acyl coenzyme A in mice lacking the sterol carrier protein-2/sterol carrier protein-x gene function, Genes Dev. 12 (1998) 1189–1201.
[72] R.M. Kernstock, A.W. Girotti, Lipid transfer protein binding of unmodified natural lipids as assessed by surface plasmon resonance methodology, Anal. Biochem. 365 (2007) 111–121.
[73] J.T. Radek, D.H. Dyer, Q. Lan, Effects of mutations in *Aedes aegypti* sterol carrier protein-2 on the biological function of the protein, Biochemistry 49 (2010) 7532–7541.
[74] S.L. Black, W.A. Stanley, F.V. Filipp, M. Bhairo, A. Verma, O. Wichmann, M. Sattler, M. Wilmanns, C. Schultz, Probing lipid- and drug-binding domains with fluorescent dyes, Bioorg. Med. Chem. 16 (2008) 1162–1173.
[75] F. Schroeder, M.E. Dempsey, R.T. Fischer, Sterol and squalene carrier protein interactions with fluorescent delta 5,7,9(11)-cholestatrien-3 beta-ol, J. Biol. Chem. 260 (1985) 2904–2911.
[76] F. Schroeder, P. Butko, G. Nemecz, T.J. Scallen, Interaction of fluorescent delta 5,7,9(11),22-ergostatetraen-3 beta-ol with sterol carrier protein-2, J. Biol. Chem. 265 (1990) 151–157.
[77] R.T. Fischer, M.S. Cowlen, M.E. Dempsey, F. Schroeder, Fluorescence of delta 5,7,9(11),22-ergostatetraen-3 beta-ol in micelles, sterol carrier protein complexes, and plasma membranes, Biochemistry 24 (1985) 3322–3331.
[78] S.M. Colles, J.K. Woodford, D. Moncecchi, S.C. Myers-Payne, L.R. McLean, J.T. Billheimer, F. Schroeder, Cholesterol interaction with recombinant human sterol carrier protein-2, Lipids 30 (1995) 795–803.
[79] K.C. Krebs, Q. Lan, Isolation and expression of a sterol carrier protein-2 gene from the yellow fever mosquito, *Aedes aegypti*, Insect Mol. Biol. 12 (2003) 51–60.
[80] N.A. Avdulov, S.V. Chochina, U. Igbavboa, C.S. Warden, F. Schroeder, W.G. Wood, Lipid binding to sterol carrier protein-2 is inhibited by ethanol, Biochim. Biophys. Acta 1437 (1999) 37–45.
[81] N. Stolowich, A. Frolov, A.D. Petrescu, A.I. Scott, J.T. Billheimer, F. Schroeder, Holosterol carrier protein-2. (13)C NMR investigation of cholesterol and fatty acid binding sites, J. Biol. Chem. 274 (1999) 35425–35433.
[82] B. Lige, B. Jayabalasingham, H. Zhang, M. Pypaert, I. Coppens, Role of an ancestral d-bifunctional protein containing two sterol-carrier protein-2 domains in lipid uptake and trafficking in toxoplasma, Mol. Biol. Cell 20 (2009) 658–672.
[83] T.W.J. Gadella, K.W. Wirtz, Phospholipid binding and transfer by the nonspecific lipid-transfer protein (sterol carrier protein 2). A kinetic model, Eur. J. Biochem. 220 (1994) 1019–1028.
[84] C. Jatzke, H.J. Hinz, U. Seedorf, G. Assmann, Stability and binding properties of wild-type and c17s mutated human sterol carrier protein 2, Biochim. Biophys. Acta 1432 (1999) 265–274.
[85] B.P. Atshaves, J.R. Jefferson, A.L. McIntosh, A. Gallegos, B.M. McCann, K.K. Landrock, A.B. Kier, F. Schroeder, Effect of sterol carrier protein-2 expression on sphingolipid distribution in plasma membrane lipid rafts/caveolae, Lipids 42 (2007) 871–884.
[86] M. Kim, V. Wessely, Q. Lan, Identification of mosquito sterol carrier protein-2 inhibitors, J. Lipid Res. 46 (2005) 650–657.
[87] D.M. Anstrom, X. Zhou, C.N. Kalk, B. Song, Q. Lan, Mosquitocidal properties of natural product compounds isolated from Chinese herbs and synthetic analogs of curcumin, J. Med. Entomol. 49 (2012), 350-355.T. .